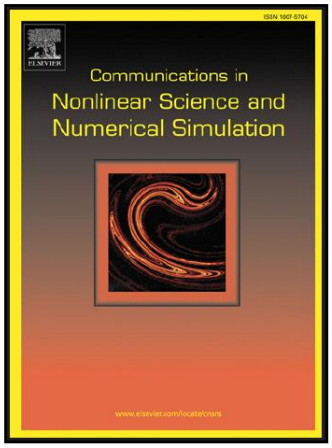

Chaos as the hub of systems dynamics. The part I – The attitude control of spacecraft by involving in the heteroclinic chaos

Anton V. Doroshin

PII: S1007-5704(17)30382-9
DOI: 10.1016/j.cnsns.2017.11.008
Reference: CNSNS 4365

To appear in: *Communications in Nonlinear Science and Numerical Simulation*

Received date: 26 May 2017
Revised date: 2 November 2017
Accepted date: 6 November 2017

Please cite this article as: Anton V. Doroshin , Chaos as the hub of systems dynamics. The part I – The attitude control of spacecraft by involving in the heteroclinic chaos, *Communications in Nonlinear Science and Numerical Simulation* (2017), doi: 10.1016/j.cnsns.2017.11.008

Chaos as the hub of systems dynamics. The part I – The attitude control of spacecraft by involving in the heteroclinic chaos

ANTON V. DOROSHIN
Space Engineering Department
(Division of Flight Dynamics and Control Systems)
Samara National Research University

Moskovskoe shosse 34, Samara, Russian Federation 443086
doran@inbox.ru; doroshin@ssau.ru; www.doroshin.ssau.ru

Abstract: - In this work the chaos in dynamical systems is considered as a positive aspect of dynamical behavior which can be applied to change systems dynamical parameters and, moreover, to change systems qualitative properties. From this point of view, the chaos can be characterized as a hub for the system dynamical regimes, because it allows to interconnect separated zones of the phase space of the system, and to fulfill the jump into the desirable phase space zone. The concretized aim of this part of the research is to focus on developing the attitude control method for magnetized gyrostat-satellites, which uses the passage through the intentionally generated heteroclinic chaos. The attitude dynamics of the satellite/spacecraft in this case represents the series of transitions from the initial dynamical regime into the chaotic heteroclinic regime with the subsequent exit to the final target dynamical regime with desirable parameters of the attitude dynamics.

Key-Words: - Satellite; Gyrostat; Dual-Spin Spacecraft; Magnetic Torque; Small Perturbations; Heteroclinic Chaos

Introduction

Ich sage euch: man muß noch Chaos in sich haben,
um einen tanzenden Stern gebären zu können.
Ich sage euch: ihr habt noch Chaos in euch.

Friedrich Nietzsche,
"Also sprach Zarathustra:
Ein Buch für Alle und Keinen"

The dynamical chaos with its properties and features is well-known important phenomenon studied by the modern science in the fundamental exploration [1-6, 13-14, 24-26, 31-33, 37-39, 42-49, 51-60] and in the broadly presented area of applications [7-23, 27-30, 34-36, 40-44]. Starting from works of Jules Henri Poincaré [51] the idea of complex behavior of dynamical systems was developed in different formulations, containing, certainly, qualitative theory of ordinal differential equations by Andronov A.A., Vitt E.A. and Khaiken S.E. [1], the theory of strange chaotic attractors, initiated by Edward Lorenz [43], the KAM-theory by Kolmogorov A.N., Arnold V.I., Moser J. [3-5, 31, 46], the Poincaré-Arnold-Melnikov-methodology for the transverse homoclinic points detection and homoclinic splitting analysis [3, 45], including its multidimensional versions developed by Wiggins S., Holmes P.J., Marsden J.E. [26, 57], and many other important aspects and research results together with problems of the integrability in nonlinear dynamics [6, 32, 33, 55], the chaos control [13-16, 25-27], and the synchronization in chaotic systems [14, 49].

The chaos in the role of irregular perturbations usually is considered as the negative aspect of systems dynamics and as the harmful process. Therefore, practically in all applied tasks it is needed to try to eliminate the dynamical chaos or to suppress its action on main dynamical properties [7-12, 15-23,

PREPRINT 10.1016/j.cnsns.2017.11.008

26-29, 34-36, 40, 41, 48-50].

In the contrast to typical negative assessments of systems chaotic behavior, in the presented paper the dynamical chaos is explored in its positive content as the dynamical instrument, which can change and improve systems dynamics in the qualitative and quantitative sense.

It is well-known fact that phase spaces (phase portraits and/or their cross-sections) of unperturbed dynamical systems represent sets of phase trajectories in the shape of separable regular curves without (self)intersections. At the action of perturbations, these regular sets are supplemented by irregular complex tangles of phase trajectories, including homo-/heteroclinic nets, which produce so-called chaotic layers. Figuratively speaking, phase spaces of perturbed dynamical systems contain “islands” of regularity and chaotic “seas” [12, 54]. It is worth to remind, that in cases of the perturbations deactivation the overwhelming majority of dynamical systems return to their natural unperturbed and fully deterministic dynamics (first of all, this refers to Hamiltonian systems). In other words, the deactivation of perturbations “desiccates chaotic seas” and the system phase point falls into the regular region on “the seabed” of unperturbed phase portrait.

This structure of the perturbed phase space theoretically allows to transport the phase point into any phase region “by the surface of the chaotic sea” crossing separated and impenetrable phase trajectories on the corresponded “seabed” of the unperturbed phase portrait. So, it is possible to consider the chaos as a hub connected separated zones of the unperturbed phase space/portrait. Through this hub the systems dynamics can sometime reach any desired “island” of regularity, because in this chaotic case the phase point forms the complex chaotic phase trajectory, which visits all positions of the available phase volume of the chaotic sea due to dynamical mixing properties.

The indicated creation of the chaos in its concrete technical implementation can be realized by system’s available dynamical actuators and special techniques of the system control. This intentional chaotization of the system dynamics is possible, for example, by the way of the transition of the phase trajectory closer to the separatrix (in the homo/heteroclinic area) with subsequent initiating harmonic perturbations in the motion parameters by available actuators [19, 20]. In addition to the homo/heteroclinic technique, the chaotization can be realize by the second way with the help of the intentional creation of strange chaotic attractors into systems dynamics with the help of available actuators [20]. Here we ought to note, that described ways of the chaotization allow not only instantaneous enable the chaos in the system, but also instantaneous disable it at any time.

Summing up above-mentioned statements, we are ready to offer the method of positive using chaos to change the system dynamical parameters in quantitative and qualitative aspects. This method is based on the intentional chaos creation with the subsequent achievement of desirable dynamical parameters in the framework of the chaotic dynamics implementation, and with instantaneous disabling the chaos after this achievement. As the result, after the passage through the chaos we will have a new dynamical behavior and a new dynamical quality of the system obtained due to the natural properties of chaos, as it is figuratively, but meaningful sounded by Friedrich Nietzsche in the epigraph. Then the main algorithm of this method are defined by the following conceptual steps (fig.1):

1. The initial step (#1): the system starts its dynamics in some initial regular regime.

2. The intermediate step (#2): the chaos into the system dynamics is intentionally initiated by the control system with the help of the special dynamical technique, so the system is intentionally “jump into the chaos” and implements the chaotic motion with the expectation of desirable parameters and the fulfillment of required criteria, which are tracked by the control system.

3. The final step (#3): At the satisfaction of necessary criteria, the control system immediately switches off the chaos, and the system proceeds to the new desired regular regime.

As can we see, in the framework of the suggested method the dynamical chaos represents the positive dynamical opportunity, which allows to proceed to the extended dynamics linking separated phase-regions in the phase space, so it is possible to characterize the dynamical chaos as *the hub of systems dynamics*. From the philosophical point of view, this interconnecting role of the chaos is very important theme of scientific research.

We can locally conclude that chaos is not only a harmful dynamical phenomenon, but also it is an opportunity; and, moreover, chaos is the hub of opportunities.

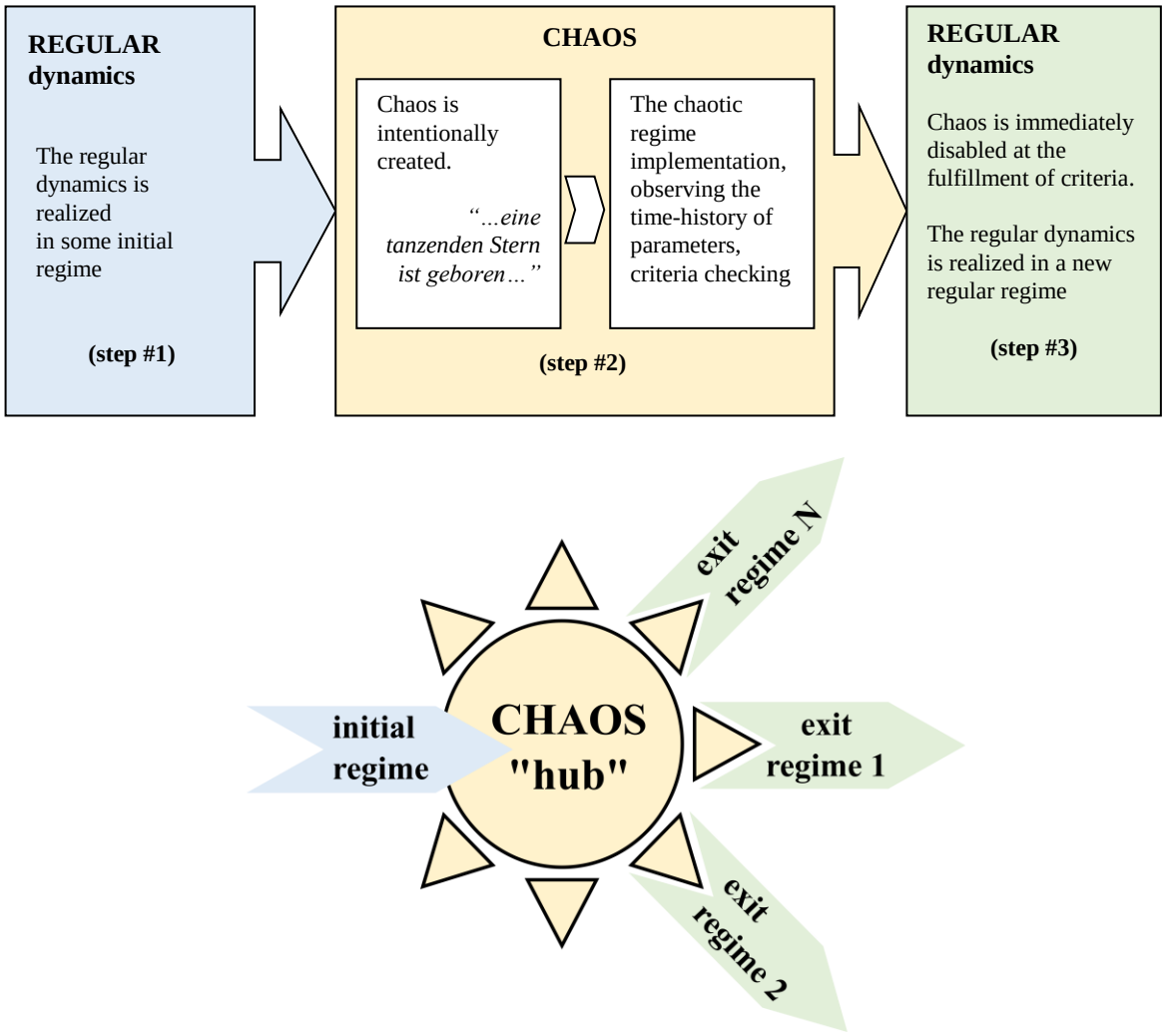

Fig.1 – *The schematic algorithm of positive using chaos to change the system dynamics*

In the next sections of the paper, the concretized scheme of the "chaotic" attitude control of magnetized gyrostat-satellites is developed, which uses the passage through the intentionally generated *homo/heteroclinic chaos*. This type of chaos in fact was fundamentally predicted in the work of Poincaré [51], and also were described in applied tasks of spacecraft (SC) attitude dynamics in many works, e.g. [12, 17-21, 27-29].

The attitude dynamics of the satellite/spacecraft at the heteroclinic "chaotic" control represents the series of transitions from the initial dynamical regime (the initial area of the phase space with initial values of angular velocities and spatial angles) to the perturbed heteroclinic regime with the subsequent exit into the final target dynamical regime (the final area of the phase space with target values of angular velocities and spatial angles). The transitional heteroclinic perturbed regime is created by the gyrostat-rotor spinup-procedure with corresponding passage of dynamics into the heteroclinic area of the phase

space and with enabling perturbations of own magnetic dipole moment of the satellite/spacecraft in the harmonic form by the magnetic torquer. This harmonic magnetic dipole moment interacts with the geomagnetic field, which, in its turn, produces the heteroclinic chaos as the positive dynamical regime, which allows to fulfill the desirable spatial reorientation of the satellite. After the destination of the target area of the dynamical phase space the harmonic magnetic perturbation turns off, and then the final motion of the satellite will remain in this final area of the phase space with target values of angular velocities and spatial angles.

As it will be shown in the next section, the suggested chaotic control scheme in the technical sense can be realized by the way of simple actuators using [19, 20]: there is needed only one longitudinal reaction wheel (with the controlled rotation velocity) and a simple "perturbing" device for the creation of internal harmonic torques, which initiates the heteroclinic chaos. In the role of this "perturbing" device it is possible to use the same reaction wheel's electromotor or the simple magnetic actuator. This constructional/functional simplicity defines the possibility of real applications of the chaotic control scheme as attitude control systems even for simplest and smallest types of SC, including nanosatellites.

Moreover, the chaotic control scheme can be also selected as the backup attitude control system for the salvation of space missions of full-featured spacecraft/satellites, which could be activated in cases of failures of the main control system, when chances of the main system recovering are lost. In these accidents, the chaotic control scheme could provide quite acceptable regimes of the further operation of the rescued SC.

1. Mechanical and mathematical models

The considered task of the realization of the chaotic control of SC is based on the well-known mechanical and mathematical models of the attitude dynamics of the rigid body with the internal rotor (coaxial bodies; dual-spin spacecraft; one-rotor gyrostat) contained magnetic actuators (magnetic torquers). The internal rotor's angular velocity can be controlled by the electro-engine. This electromotor can be used for the spin-up/spin-down of the rotor relatively the main body, and also it can produce the harmonic torque for the initiation of the perturbations of the angular velocity. The magnetic actuator generates the own dipole magnetic moment of the SC to interact with the external (geo)magnetic field and to create the external torque. These magnetic actuators controlled by the control system can form the harmonic time-dependencies of the vector of the own dipole magnetic moment.

The schematic structure of the SC and the necessary coordinates frames are presented at the figure (fig.2). The main coordinates frames include the inertial frame *CXYZ* and the frame *Cxyz* connected with the main body of SC. The inertial axis *CZ* is selected/defined along the initial unperturbed position of the vector of the system angular momentum **K**; at that the rotor-body has the absolute longitudinal angular momentum **Δ**.

In the framework of our research, we describe the motion of the SC as the series of the free motion regular regimes and the chaotic intermediate regimes, which can be created with the help of small perturbed torques formed by the actuators (the internal electromotor of the rotor-body and the magnetic torquer).

The magnetic torquer produces the control torque as the result of the interaction of the own magnetic dipole moment of the SC (**m**) with the external (geo)magnetic field (with the corresponding magnetic induction vector $\mathbf{B}_{orb}$):

$$\mathbf{M}_{ctrl} = \mathbf{m} \times \mathbf{B}_{orb} \tag{1.1}$$

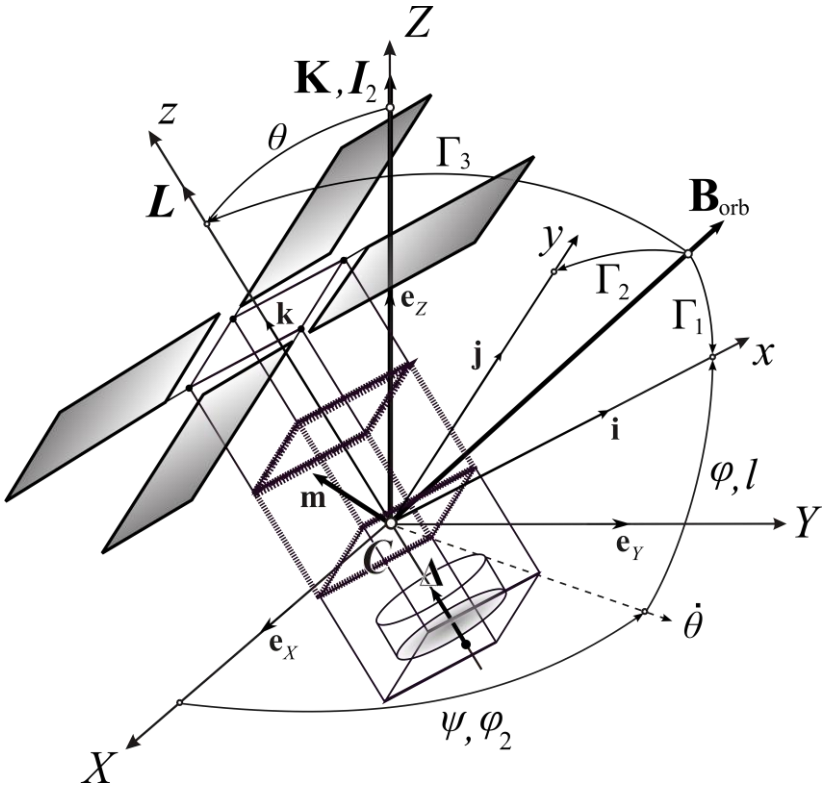

Fig.2 – *The SC schematic construction and coordinates systems*

Let us consider the vector $\mathbf{B}_{orb}$ as the constant vector in the inertial space due to consideration of the task on the short segment of the orbital motion, and, therefore, the components of this vector in inertial frame *CXYZ* are constant $\mathbf{B}_{orb}=[B_X, B_Y, B_Z]^T$. The direction of the vector of the magnetic induction $\mathbf{B}_{orb}$ of the external field in the connected frame *Cxyz* we will describe by the directional cosines $\Gamma_1=\cos(\mathbf{B}_{orb},\mathbf{i})$, $\Gamma_2=\cos(\mathbf{B}_{orb},\mathbf{j})$, $\Gamma_3=\cos(\mathbf{B}_{orb},\mathbf{k})$. Then we can write the following components of the magnetic induction vector $\mathbf{B}_{orb}$, the magnetic dipole moment $\mathbf{m}$ and the control torque in the connected coordinates frame *Cxyz*:

$$\begin{aligned}&\mathbf{B}_{orb}=B_{orb}\left[\Gamma_1,\Gamma_2,\Gamma_3\right]^T; \qquad \mathbf{m}=\left[m_x(t),m_y(t),m_z(t)\right]^T;\\ &\mathbf{M}_{ctrl}=B_{orb}\left[m_y\Gamma_3-m_z\Gamma_2;\ \ m_z\Gamma_1-m_x\Gamma_3;\ \ m_x\Gamma_2-m_y\Gamma_1\right]^T\end{aligned} \tag{1.2}$$

The motion equations of the SC with one internal rotor-body can be written in the vector form [17] together with the kinematical equations for the directional cosines (relatively the connected axes *Cxyz*) for the unit vectors $\{\mathbf{e}_X, \mathbf{e}_Y, \mathbf{e}_Z\}$ of the inertial coordinates system *CXYZ* $\{\alpha_i, \beta_i, \gamma_i\}$, and for directional cosines $\{\Gamma_i\}$ of the constant vector $\mathbf{B}_{orb}$:

$$\frac{\tilde{d}}{dt}\mathbf{K}+\boldsymbol{\omega}\times\mathbf{K}=\mathbf{M}_{ctrl}; \qquad \dot{\Delta}=M_{internal} \tag{1.3}$$

$$\left\{\begin{matrix}\dot{\boldsymbol{\alpha}}=\boldsymbol{\alpha}\times\boldsymbol{\omega}; & \dot{\boldsymbol{\beta}}=\boldsymbol{\beta}\times\boldsymbol{\omega};\\ \dot{\boldsymbol{\gamma}}=\boldsymbol{\gamma}\times\boldsymbol{\omega}; & \dot{\boldsymbol{\Gamma}}=\boldsymbol{\Gamma}\times\boldsymbol{\omega}\end{matrix}\right\} \tag{1.4}$$

where $M_{internal}-$ is the value of the internal longitudinal torque acting on the rotor from the side of the

main body through the electromotor.

The angular momentum **K** and the longitudinal (along the *Cz*) angular momentum of the rotor-body have the following projections on axes of the connected frame *Cxyz*:

$$\mathbf{K} = \left[Ap,\ Bq,\ C_b r + \Delta \right]^T; \quad \Delta = C_r \left(r + \sigma \right) \tag{1.5}$$

Here $A = A_b + A_r$, $B = B_b + A_r$; and $\left\{ A_b, B_b, C_b \right\}$ correspond to the axial inertia moments of the main SC body in the connected frame *Cxyz*; and $\left\{ A_r, A_r, C_r \right\}$ represent the axial inertia moments of the dynamically symmetrical rotor in its own connected frame; $[p, q, r]^{\mathrm{T}}$ – are components of the vector of the angular velocity of the main body in the connected frame *Cxyz*, σ – is the angular velocity of the rotor rotation relative the main body (along the *Cz*). Let us assume that $A_b > B_b > C_b > A_r > C_r$.

The main dynamical equations of the SC attitude motion have the form:

$$\begin{cases} A\dot{p} + \left(C_b - B \right) qr + q\Delta = B_{orb} \left(m_y \Gamma_3 - m_z \Gamma_2 \right); \\ B\dot{q} + \left(A - C_b \right) pr - p\Delta = B_{orb} \left(m_z \Gamma_1 - m_x \Gamma_3 \right); \\ C_b \dot{r} + \dot{\Delta} + pq \left(B - A \right) = B_{orb} \left(m_x \Gamma_2 - m_y \Gamma_1 \right); \\ \dot{\Delta} = M_{internal} \end{cases} \tag{1.6}$$

The well-known Euler angles (fig.2) also will be used in this research; the corresponding kinematical equations for the Euler angles have the form:

$$\begin{cases} \dot{\theta} = p\cos\varphi - q\sin\varphi; \\ \dot{\psi} = (p\sin\varphi + q\cos\varphi)/\sin\theta; \\ \dot{\varphi} = r - \mathrm{ctg}\,\theta (p\sin\varphi + q\cos\varphi) \end{cases} \tag{1.7}$$

As it already were indicated above, the magnetic control torque and the internal torque $M_{internal}$ are formed by the actuators as perturbing dynamical factors for the creation of the intermediate chaotic regime, connected the initial and final regimes of the SC free motion. Moreover, we define these perturbations in the simplest harmonic form, which can be easy realized by the actuators. So, these torques, firstly, are small and, secondly, are limited in time of their operation during the chaotic regime implementation, that mathematically is expressed as follows:

$$\begin{cases} m_i \left(t \right) = \mu_i \left[\mathrm{H}\left(t - t_{start} \right) - \mathrm{H}\left(t - t_{finish} \right) \right] \sin\left(\Omega_i t \right); \\ \\ M_{internal} \left(t \right) = \mu_\Delta \left[\mathrm{H}\left(t - t_{start} \right) - \mathrm{H}\left(t - t_{finish} \right) \right] \cos\left(\Omega_\Delta t \right), \end{cases} \tag{1.8}$$

where μ_i, μ_Δ are small values of corresponding perturbing factors (i=x, y, z); Ω_Δ and Ω_i are frequencies of harmonic perturbations; H(t) is the is the Heaviside function; t_{start} and t_{finish} are the time-points of the perturbations enabling and disabling. We should note, that for the chaos creation we can use the both perturbing factors (μ_i, μ_Δ) together and/or separately one of them.

2. The canonical form of the dynamical model in the Serret-Andoyer-Deprit variables

Let us build the Hamiltonian form of equations using the well-known [e.g. 32, 33] canonical Serret-Andoyer-Deprit variables ($\{\varphi_3, I_3\}$, $\{\varphi_2, I_2\}$, $\{l, L\}$):

$$L = \frac{\partial T}{\partial \dot{l}} = \mathbf{K}\cdot\mathbf{k}; \quad I_2 = \frac{\partial T}{\partial \dot{\varphi}_2} = \mathbf{K}\cdot\frac{\mathbf{K}}{K} = |\mathbf{K}| = K; \quad I_3 = \frac{\partial T}{\partial \dot{\varphi}_3} = \mathbf{K}\cdot\mathbf{k}' \tag{2.1}$$

We already assume the relative smallness of the magnetic torque (1.1) (as it follows from (1.8) inside the time-interval $[t_{start}, t_{finish}]$). Then in the generating case (at the formal consideration of the dynamics without any perturbations) the angular momentum **K** will be constant vector of the torque-free motion. In our case (when the vector **K** is co-directional with *CZ*) the canonical variables reduce to two pares ($\{\varphi_2, I_2\}$, $\{l, L\}$) that is depicted at the fig.2, and the following correspondences with the Euler angles are fulfilled:

$$\begin{cases} l = \varphi; \quad \varphi_2 = \psi; \quad \varphi_3 = 0; \\ I_2 = K; \quad \cos\theta = L/I_2 = L/K; \\ \sin\theta = \sqrt{I_2^2 - L^2}\,/I_2 = \sqrt{K^2 - L^2}\,/K \end{cases} \tag{2.2}$$

The angular momentum components are linked with the canonical momentums as follows:

$$K_x = Ap = \sqrt{I_2^2 - L^2}\sin l; \quad K_y = Bq = \sqrt{I_2^2 - L^2}\cos l; \quad K_z = C_b r + \Delta = L \tag{2.3}$$

The Hamiltonian of the system has the following form in the Serret-Andoyer–Deprit variables:

$$\begin{aligned} &\mathcal{H} = \mathcal{H}_0 + \varepsilon\mathcal{H}_1; \qquad \mathcal{H}_0 = T_0 + P_0; \qquad \varepsilon\mathcal{H}_1 = \varepsilon T_1 + \varepsilon P_1; \\ &T_0 = \frac{I_2^2 - L^2}{2}\left[\frac{\sin^2 l}{A} + \frac{\cos^2 l}{B}\right] + \frac{1}{2}\left[\frac{\Delta^2}{C_r} + \frac{(L-\Delta)^2}{C_b}\right]; \; P_0 = 0; \end{aligned} \tag{2.4}$$

where T_0 is the expression for the kinetic energy (for the unperturbed system), P_0 is the part of the potential energy (in the framework of this consideration it is equal to zero), and $\varepsilon\mathcal{H}_1$ – is the small part of the Hamiltonian which describes possible small (proportional to the small parameter ε) perturbations acting on the system. To write the expressions for the perturbed part of the potential energy it is needed to consider the magnitude of the magnetic torque (1.1) with integrating it by the corresponding positional angle $\vartheta = \angle(\mathbf{m}, \mathbf{B}_{orb})$ - it is possible by the way of the evaluation of the scalar production of vectors through the components in the inertial frame:

$$\begin{aligned} &|\mathbf{M}_{ctrl}| = |\mathbf{m}\times\mathbf{B}_{orb}| = |\mathbf{m}||\mathbf{B}_{orb}|\sin\vartheta; \\ &\varepsilon P_1 = -\int |\mathbf{M}_{ctrl}|\,d\vartheta = -|\mathbf{m}||\mathbf{B}_{orb}|\cos\vartheta = -\mathbf{m}\cdot\mathbf{B}_{orb} = \\ &= -\left\{\begin{bmatrix} \alpha_1 & \alpha_2 & \alpha_3 \\ \beta_1 & \beta_2 & \beta_3 \\ \gamma_1 & \gamma_2 & \gamma_3 \end{bmatrix}\cdot\begin{bmatrix} m_x \\ m_y \\ m_z \end{bmatrix}\right\}\cdot\begin{bmatrix} B_X \\ B_Y \\ B_Z \end{bmatrix} \end{aligned} \tag{2.5}$$

In the considered research, when the axis *CZ* coincides with the generating (unperturbed) vector of the angular momentum **K**, using (2.2) and well-known expressions for the Euler angles, the following expressions for the directional cosines through the Serret-Andoyer–Deprit variables can be written:

$$\begin{cases} \begin{cases} \alpha_1 = \cos\varphi\cos\psi - \cos\theta\sin\psi\sin\varphi = \cos l\cos\varphi_2 - \left(L/I_2\right)\sin\varphi_2\sin l; \\ \alpha_2 = -\sin\varphi\cos\psi - \cos\theta\sin\psi\cos\varphi = -\sin l\cos\varphi_2 - \left(L/I_2\right)\sin\varphi_2\cos l; \\ \alpha_3 = \sin\theta\sin\psi = \left(\sqrt{I_2^2 - L^2}\,/I_2\right)\sin\varphi_2; \end{cases} \\ \begin{cases} \beta_1 = \cos\varphi\sin\psi + \cos\theta\cos\psi\sin\varphi = \cos l\sin\varphi_2 + \left(L/I_2\right)\cos\varphi_2\sin l; \\ \beta_2 = -\sin\varphi\sin\psi + \cos\theta\cos\psi\cos\varphi = -\sin l\sin\varphi_2 + \left(L/I_2\right)\cos\varphi_2\cos l; \\ \beta_3 = -\sin\theta\cos\psi = -\left(\sqrt{I_2^2 - L^2}\,/I_2\right)\cos\varphi_2; \end{cases} \\ \begin{cases} \gamma_1 = \sin\theta\sin\varphi = \left(\sqrt{I_2^2 - L^2}\,/I_2\right)\sin l; \\ \gamma_2 = \sin\theta\cos\varphi = \left(\sqrt{I_2^2 - L^2}\,/I_2\right)\cos l; \\ \gamma_3 = \cos\theta = L/I_2 \end{cases} \end{cases} \tag{2.6}$$

Then the perturbed part of the potential energy (2.5) described by the Serret-Andoyer-Deprit variables can be obtained with the help of connections (2.6):

$$\varepsilon P_1\left(l, L, \varphi_2, I_2\right) = -m_x\left\{\alpha_1 B_X + \beta_1 B_Y + \gamma_1 B_Z\right\} - m_y\left\{\alpha_2 B_X + \beta_2 B_Y + \gamma_2 B_Z\right\} - m_z\left\{\alpha_3 B_X + \beta_3 B_Y + \gamma_3 B_Z\right\} \tag{2.7}$$

Let us, however, to consider a particular case of the magnetic perturbation when the own dipole magnetic moment **m** has only one longitudinal component m_z. It is quite enough for solving the problem of the motion intentional chaotization. Then the following perturbed part of the potential takes place:

$$\varepsilon P_1 = -\frac{m_z}{I_2}\left[\sqrt{I_2^2 - L^2}\left(B_X\sin\varphi_2 - B_Y\cos\varphi_2\right) + B_Z L\right] \tag{2.8}$$

If we take into account the action (inside the time-interval [t_{start}, t_{finish}] of the perturbed motion) of the harmonic perturbation from the internal rotor engine, then the solution for perturbed angular momentum $\tilde{\Delta}$ of the rotor-body follows after independent integrating the last equation (1.6):

$$\tilde{\Delta}\left(t\right) = \Delta + \frac{\mu_\Delta}{\Omega_\Delta}\sin\left(\Omega_\Delta t\right) \tag{2.9}$$

The substitution of the solution (2.9) into the expression for the Hamiltonian (2.4) rejecting terms of the second order $O\left(\mu^2\right)$ gives the perturbed part of the kinetic energy:

$$\varepsilon T_1 = \frac{\mu_\Delta}{\Omega_\Delta}\sin\Omega_\Delta t\left[\frac{\Delta}{C_r}-\frac{L-\Delta}{C_b}\right] \tag{2.10}$$

Expressions (2.10) and (2.8) define the perturbed part of the Hamiltonian of the perturbed motion with the simplest intentional harmonic perturbations in the magnetic dipole and in the internal rotor's engine, that is fulfilled with the aim of the intentional chaos creation. Then it is possible to write the equations for the canonical Serret-Andoyer-Deprit variables, which describe the perturbed dynamics (inside the time-interval [t_{start}, t_{finish}]):

$$\begin{cases}\dot L = f_L + \varepsilon g_L; & \begin{cases}\dot I_2 = f_{I_2} + \varepsilon g_{I_2};\\ \dot\varphi_2 = f_{\varphi_2} + \varepsilon g_{\varphi_2};\end{cases}\\ \dot l = f_l + \varepsilon g_l; & \end{cases} \tag{2.11}$$

where

$$\begin{cases}\begin{cases} f_L = -\frac{1}{2}\left[I_2^2 - L^2\right]\left(\frac{1}{A}-\frac{1}{B}\right)\sin(2l); \qquad f_l = L\left[\frac{1}{C_b}-\frac{\sin^2 l}{A}-\frac{\cos^2 l}{B}\right]-\frac{\Delta}{C_b};\\ \varepsilon g_L = 0;\ \varepsilon g_l = -\frac{\mu_\Delta}{\Omega_\Delta C_b}\sin\Omega_\Delta t - \frac{m_z}{I_2}\left[B_Z - \frac{L}{\sqrt{I_2^2-L^2}}\left(B_X\sin\varphi_2 - B_Y\cos\varphi_2\right)\right];\end{cases}\\ \begin{cases} f_{I_2} = 0; \qquad \varepsilon g_{I_2} = \frac{m_z}{I_2}\left[\sqrt{I_2^2-L^2}\left(B_X\cos\varphi_2 + B_Y\sin\varphi_2\right)\right];\\ f_{\varphi_2} = I_2\left[\frac{\sin^2 l}{A}+\frac{\cos^2 l}{B}\right];\quad \varepsilon g_{\varphi_2} = \frac{m_z L}{I_2^2}\left[B_Z - \frac{L}{\sqrt{I_2^2-L^2}}\left(B_X\sin\varphi_2 - B_Y\cos\varphi_2\right)\right]\end{cases}\end{cases} \tag{2.12}$$

and in view of (1.8)

$$\begin{cases}\begin{cases} f_L = -\frac{1}{2}\left[I_2^2 - L^2\right]\left(\frac{1}{A}-\frac{1}{B}\right)\sin(2l); \qquad f_l = L\left[\frac{1}{C_b}-\frac{\sin^2 l}{A}-\frac{\cos^2 l}{B}\right]-\frac{\Delta}{C_b};\\ \varepsilon g_L = 0;\ \varepsilon g_l = -\varepsilon\left\{e_\Delta\Omega_\Delta\sin\Omega_\Delta t + e_z\Omega_z\left[1-\frac{L}{\sqrt{I_2^2-L^2}}\left(b_X\sin\varphi_2 - b_Y\cos\varphi_2\right)\right]\sin(\Omega_z t)\right\};\end{cases}\\ \begin{cases} f_{I_2} = 0; \qquad \varepsilon g_{I_2} = \varepsilon e_z\Omega_z\left[\sqrt{I_2^2-L^2}\left(b_X\cos\varphi_2 + b_Y\sin\varphi_2\right)\right]\sin(\Omega_z t);\\ f_{\varphi_2} = I_2\left[\frac{\sin^2 l}{A}+\frac{\cos^2 l}{B}\right];\quad \varepsilon g_{\varphi_2} = \varepsilon e_z\Omega_z\frac{L}{I_2}\left[1-\frac{L}{\sqrt{I_2^2-L^2}}\left(b_X\sin\varphi_2 - b_Y\cos\varphi_2\right)\right]\sin(\Omega_z t)\end{cases}\end{cases} \tag{2.13}$$

where $b_X = B_X/B_Z$; $b_Y = B_Y/B_Z$ and the dimensionless small parameter ε is involved:

$$\varepsilon = \sup(\varepsilon_\Delta, \varepsilon_z);\quad \varepsilon_\Delta = \frac{\mu_\Delta}{\Omega_\Delta^2 C_b};\quad \varepsilon_z = \frac{\mu_z B_Z}{\Omega_z I_2}; \tag{2.14}$$

with the corresponding factors of the relative smallness of the perturbations $\{e_\Delta = \varepsilon_\Delta/\varepsilon;\quad e_z = \varepsilon_z/\varepsilon\}$.

At the end of this section, we present the structure of the phase space of unperturbed generating system (fig. 3) in the Serret-Andoyer-Deprit variables (fig.3-a) and in the space of the angular velocity components in the form of the so-called plhodes ellipsoid (fig.3-b) at the assumption that A_b>B_b>C_b.

The unperturbed Serret-Andoyer-Deprit phase dynamics has one noncyclic degree of freedom (as it follows from (2.11) at ε=0) and can be fully described by the phase plane $\{l, L\}$. The phase trajectories in both cases (fig. 3) represent the closed lines (tacking into account the identification of points of the Serret-Andoyer-Deprit phase trajectories at the values l=0=2π). Both types of phase spaces/portraits contain two heteroclinic points (S_1 and S_2), which are connected by the heteroclinic orbits/trajectories, which also are called as separatrices. As it is known and as it will be demonstrated in the next section, exactly these heteroclinic trajectories will split at the action of perturbations and will generate the heterocinic nets/tangles – this is the reason of the chaotic dynamics creation in the neighborhood of heteroclinic trajectories, that is called as the heteroclinic chaos.

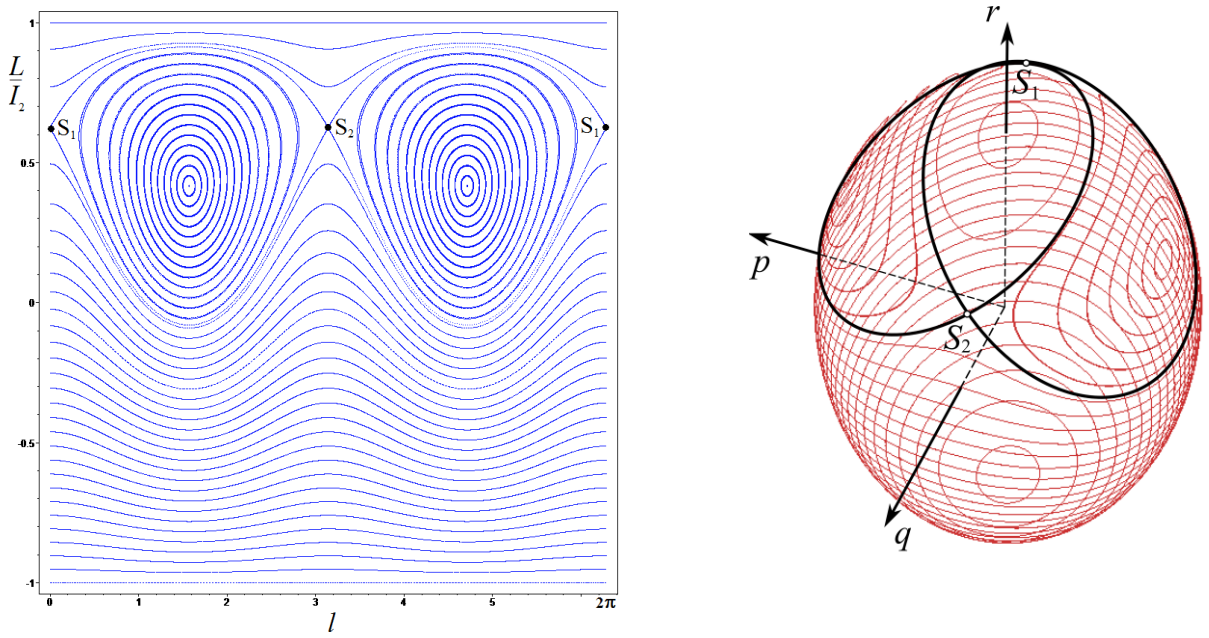

(a) (b)

Fig.3 – *The phase spaces of the generating system*

3. The preliminary numerical overview of the chaotic behavior of the perturbed system

Now it is possible to obtain some numerical results to explain main properties of the chaotic motion of the perturbed system. First of all, we will build the cross-sections of the system phase space in the Serret-Andoyer-Deprit variables. From the equations (2.11) with expressions (2.13) we can see that the system formally has two degrees of freedom ($\{\varphi_2, I_2\}$, $\{l, L\}$) at the action of both types of perturbations (1.8) (inside the time-interval [t_{start}=0, t_{finish}=∞]); and also it has the additional (fifth) dimension corresponded to the time due to the non-autonomous form of perturbations. Therefore, we need to make the well-known Poincaré-section and to analyze some projections of the phase portrait (fig.4). In this work the Poincaré-sections are plotted on the base of the "stroboscopic condition" when the points of phase trajectories are added to the phase portrait at the fulfilling the equality:

$$\mathrm{mod}\left(t, 2\pi/\Omega\right) = 0; \qquad \Omega = \sup\left(\Omega_{\Delta}, \Omega_{z}\right) \tag{3.1}$$

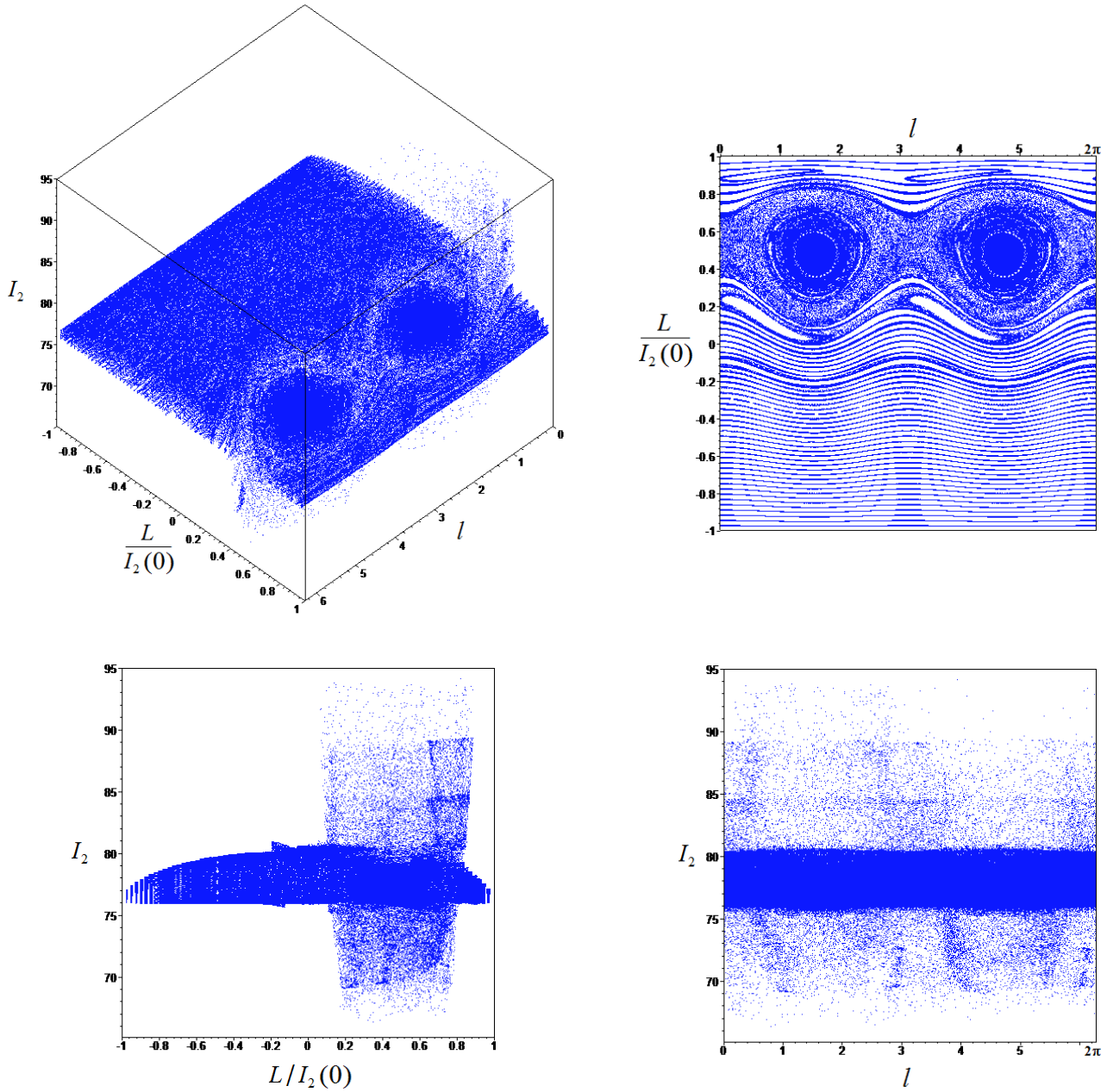

Fig.4 – *The three-dimensional Poincaré section and it's projections*

Let us present the series of Poincaré sections in projection on the plane $\{l, L/I_2(0)\}$ which contains the more important information about the phase space of the system and about the perturbed heteroclinic area (fig.5, 6). These sections are plotted in the interests of the comparative analysis of the dynamics at different perturbations and the system parameters (fig.5) presented in the table (tabl.1).

As can we see, the sections obtained at the internal perturbation action (fig.5-a, c, e, g, i) have clearly marked separations of phase zones including the primary and secondary "chaotic layers" in heteroclinic regions. In cases of external magnetic perturbations the Poincaré sections projections (fig.5-b, d, f, h) have blurred forms due to the greater dimension of the phase space in comparison with cases of internal perturbations (when forms are precise).

Undoubtedly, the presented at the figures (fig.4, 5) Poincaré sections were plotted at the hypothetical dynamical parameters (tabl.1) which conditionally and tentatively correspond to real SC and torquers. These hypothetical parameters were selected as the appropriate values for the chaotic regimes illustration and for the chaotic reorientation of SC demonstration. However, the values of dynamical parameters for the phase portrait at the fig.6 are quite applicable to the consideration of the real dynamics of small SC in the real geomagnetic field at the motion of micro-spacecraft and/or nano-satellites along the low orbit (B_{orb}~50 [μT]) with powerful magnetic torquers (m~40 [A·m^2]).

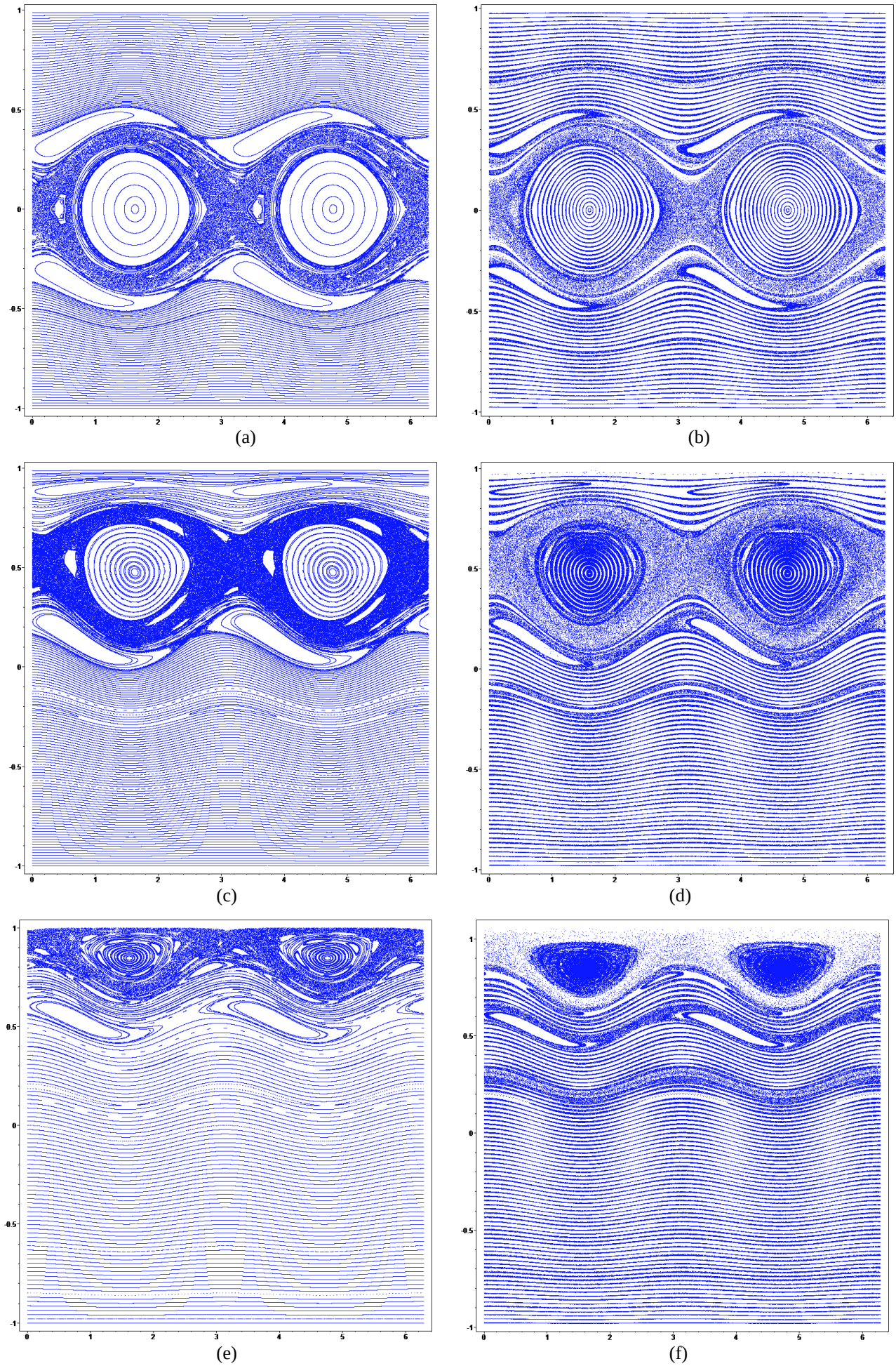

Fig.5 – *The Poincaré sections of the perturbed phase space*

PREPRINT 10.1016/j.cnsns.2017.11.008

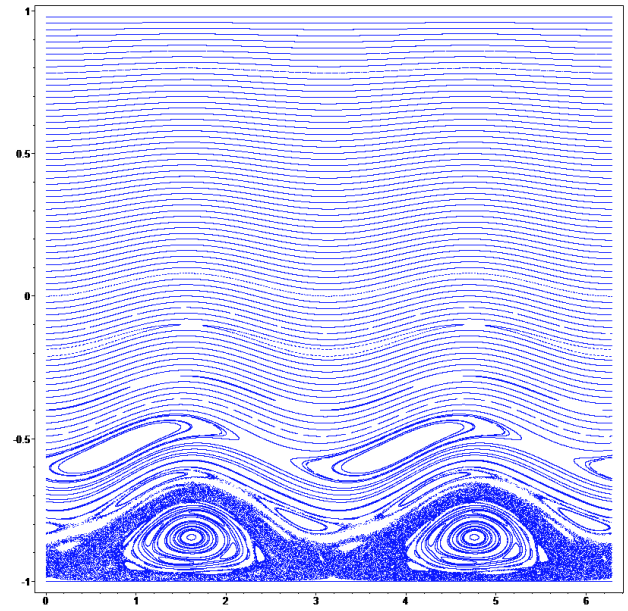

(g)

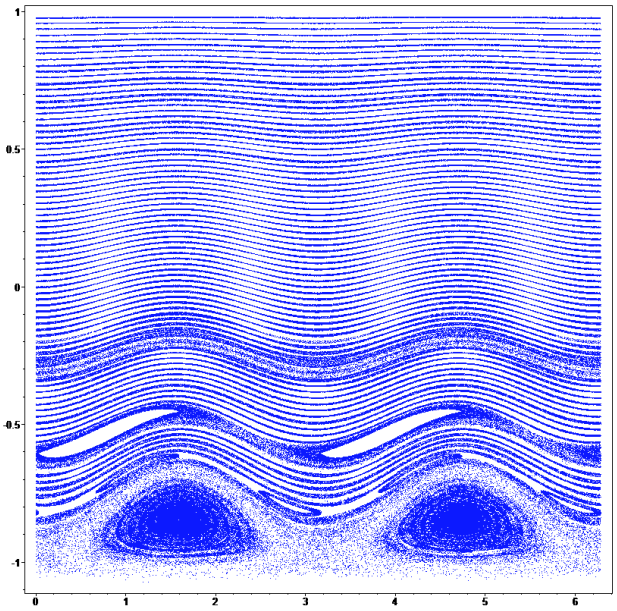

(h)

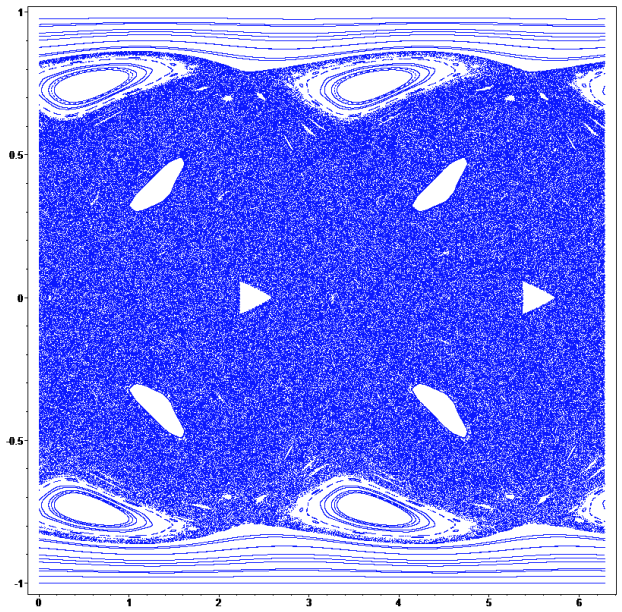

(i)

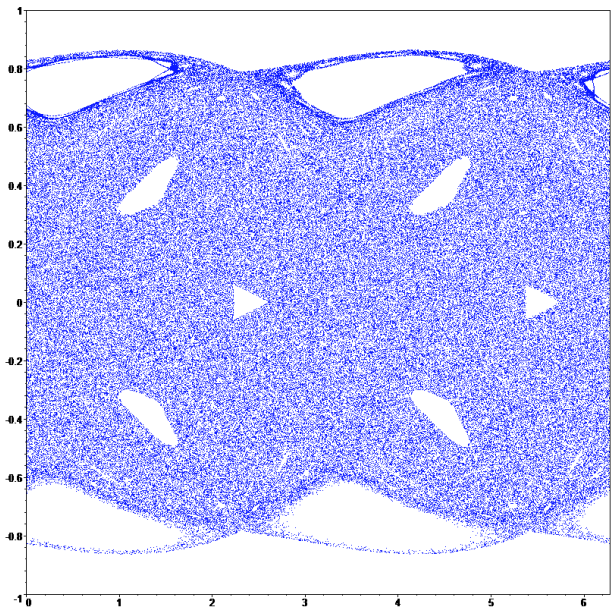

(j)

Fig.5 (continuation)

Table 1. *Parameters of the perturbed system dynamics*

Fig.	A, kg*m^2	B, kg*m^2	C_b, kg*m^2	$I_2(0)$, kg*m^2/s	Δ, kg*m^2/s	b_X	b_Y	$\mu_z B_Z$, N*m	μ_Δ, N*m	Ω_Δ, 1/s	Ω_z, 1/s
4	20	15	6	76	76/3	1/4	3/4	8	0	-	2π
5-a					0	-	-	0	10	2π	-
5-b					0	1/4	3/4	8	0	-	2π
5-c					76/3	-	-	0	10	2π	-
5-d					76/3	1/4	3/4	8	0	-	2π
5-e					45	-	-	0	10	2π	-
5-f					45	1/4	3/4	8	0	-	2π
5-g					-45	-	-	0	10	2π	-
5-h					-45	1/4	3/4	8	0	-	2π
5-i,j					0	-	-	0	150	2π	-
6-a	0.2	0.15	0.06	0.76	0	1/3	1/3	0.002	0.0	-	π/10
6-b									0.1	π	π/10
6-c,d									0.5	π	π/10

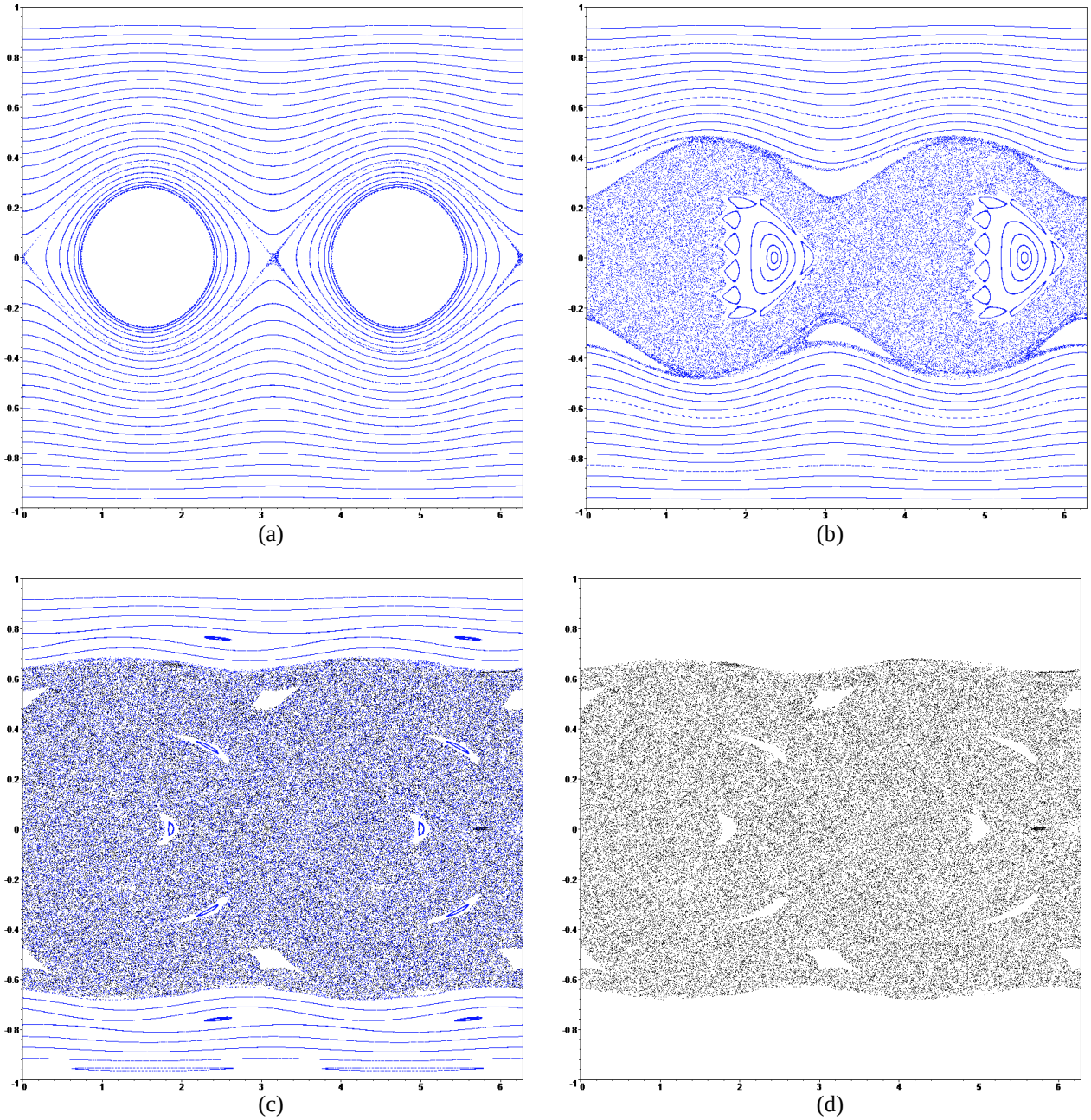

Fig.6 –*The Poincaré sections for the micro-/nano-satellite case*

Here we separately note the pair of the Poincaré sections (fig.5, fragments i and j) – these sections were obtained at the large value of the internal perturbation for the identical initial conditions and for the same dynamical parameters. The fragment (fig.5-j) contains points of one single phase trajectory started from the heteroclinic region. This perturbed phase trajectory, as can we see, passes through almost the entire accessible area of the phase space and independently of the other generates the so-called chaotic layer ("chaotic sea"). The same situation is presented at the pair of sections (fig.6, fragments c and d) for the case of micro-SC/nano-satellites. This dynamical fact confirms the possibility of the implementation of the "chaotic" attitude control described in the introduction, because in this case we have the chaotic sea linking all phase zones, which become available to all initially separated (in the unperturbed dynamics) phase trajectories "covered by this sea". In other words, each perturbed phase trajectory from this chaotic layer can arrive any linked zone of the phase space and continue new unperturbed dynamics in new dynamical regions after perturbations disabling.

In addition, it is needed to give some comments about the comparative analysis of the internal ($M_{internal}$) and external magnetic (M_{ctrl}) perturbations relatively the efficiency of the chaotic layer

creation, which is the important part of the method of the chaotic attitude control of SC (especially micro-SC/nano-satellites). From the fragment (fig.6-a) we can see, that the taken separately magnetic perturbation generates the narrow chaotic layer in the comparison with the case of the conjoint action together with the small internal perturbation (fig.6-b). This circumstance characterizes the magnetic type of perturbations as small and "slow", but quite realizable. The internal perturbations from the rotor engine undoubtedly are more fast and effective in the sense of the chaotic motion creation: the fragment (fig.6-d) shows the points of one single perturbed phase trajectory filling practically the entire volume of the phase space. So, the both types of perturbations can be applied separately or jointly to the heteroclinic chaos creation, that allows to construct the appropriate actuator for the implementation of the method of the chaotic attitude control.

4. The method of chaotic attitude control of the SC by using homo/heteroclinic chaos-hub

As it was indicated above, the chaos can be used in the role of the dynamical hub linking separated zones of systems phase spaces. Due to the natural suppleness of homo/heteroclinic regions of systems phase spaces to the dynamical chaos generation at the action of small perturbations, we can suggest the type of heteroclinic chaos as the primary simplest technique to implement the SC attitude control by the way of the "chaos-hub" creation.

In the introduction the main conceptual scheme of the chaos-hub was described in the framework of systems dynamics changing (fig.1). This general scheme can be adopted to the task of the chaotic attitude control of SC and its dynamics quality alteration [19, 20].

Primarily, let us give necessary comments about the possible angular/attitude motion of the torque-free SC with internal rotor (it also is called as the dual-spin spacecraft or the gyrostat-satellite). It is needed to emphasize four main zones ($\mathfrak{A}$-$\mathfrak{D}$) and types of the torque-free angular motion (fig.7). In addition, we should indicate separately the heteroclinic zone-$\mathfrak{H}$ (fig.7-c), which is born from the unperturbed heteroclinic trajectories S_1S_2 (fig.3) at their splitting at the action of perturbations, that produces the heteroclinc net and the corresponding chaotic layer (the "chaotic sea").

The first type of zones is the $\mathfrak{A}$-zone. In the $\mathfrak{A}$-zone the SC has the attitude dynamics usual in space missions, when its longitudinal axes (*Cz*) fulfills the rotational motion around the vector of the angular momentum **K** with oscillations relatively small values of the nutation angle θ (fig.7-d). Then the SC also rotates around the *Cz* in positive direction; so, we have the motion with the positive precession velocity ($\dot{\psi} > 0$), positive intrinsic rotation velocity ($\dot{\varphi} > 0$) and small oscillated nutation. In other words, in this mode the SC rotates preferably around its own main longitudinal axes *Cz*. This regime of the angular motion corresponds to the stabilized rotation of the SC with the conservation of the main direction of longitudinal axes – this regime is called as gyroscopic stabilization, and it represents the most efficient and desirable regime for the dual-spin spacecraft and for the gyrostat-satellite, because this regime provides the stabilization of the spatial direction of the spacecraft's equipment (antennas, telescopes, solar panels, etc.). In ideal conditions, the longitudinal axes *Cz* fully coincides with the vector of the angular momentum (then $L/I_2=1$) with the zero-value of the nutation; nevertheless, the whole $\mathfrak{A}$-zone is the quite acceptable for space-flight applications, and, in the first place, for the micro- and nano-spacecraft/satellites.

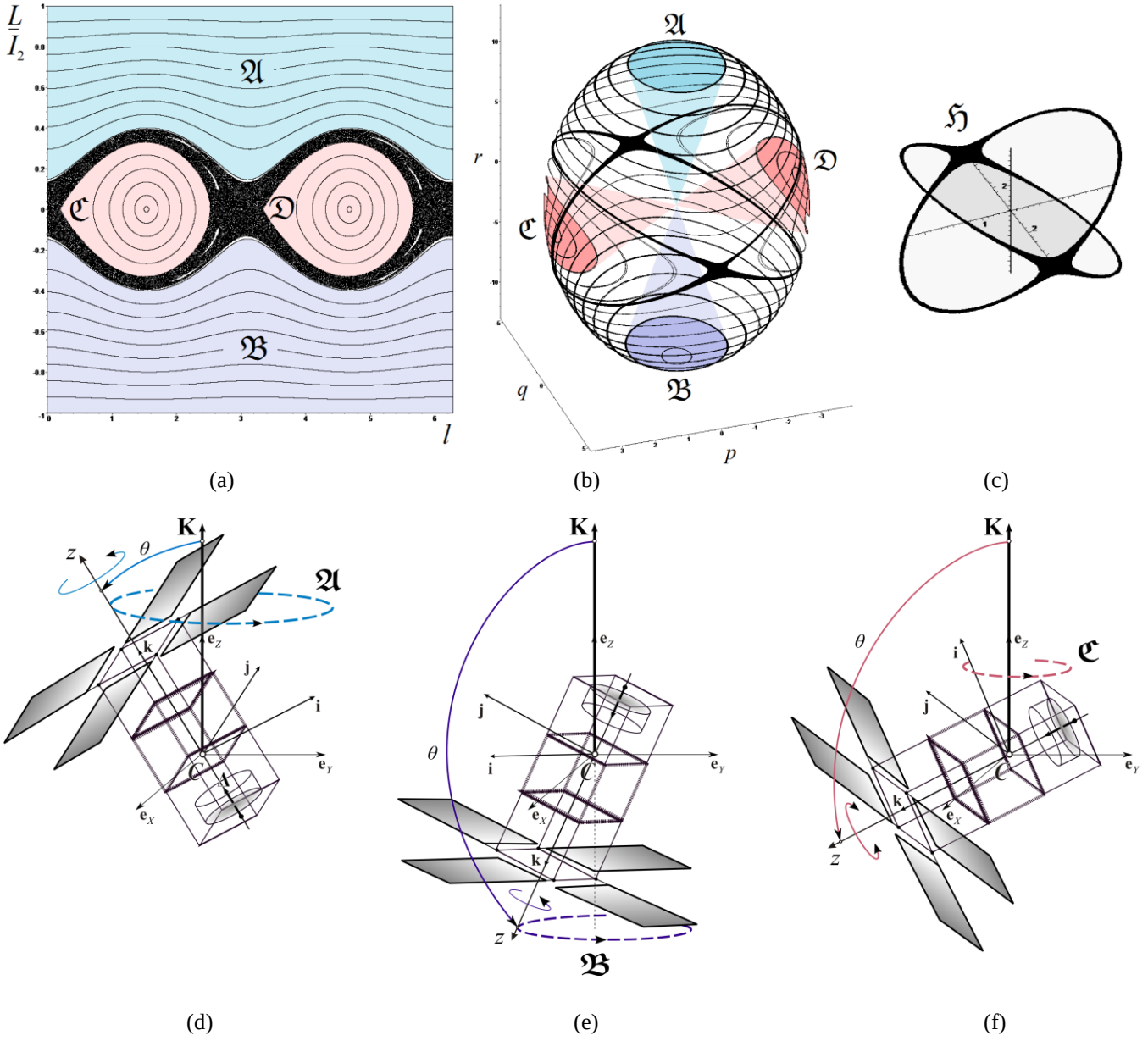

Fig.7 – *The main phase zones of the angular motion of the torque-free spacecraft*

The dynamics in the 𝔅-zone is the "antipode" to the dynamics in the 𝔄-zone, when the direction of the longitudinal axis *Cz* is opposite to the vector of the angular momentum **K** (fig.7-e), but this axis as before rotates around **K**, with blunt nutation angles. The rotation of the SC is still fulfilled preferably around its own longitudinal axes but in the negative directions, i.e. the angular motion has the positive precession velocity, the negative intrinsic rotation velocity, and substantially large values of the nutation.

For the dynamics in the 𝔈-zone we have the preferably rotation about the transversal axes *Ox*, which fulfills the positive precessional rotation around the angular momentum vector **K** (fig.7-f). The angle of intrinsic rotation in the 𝔈-zone fulfills the periodical oscillations around the value $\varphi^*=\pi/2$. So, this type of motion usually is considered as the worst regime in the sense of the spatial orientation for the spin-stabilized SC, because in this case the SC moves sideways relative the main stabilized spatial direction (the direction of **K**).

The dynamics in the $\mathfrak{D}$-zone is practically the same that the dynamics in the $\mathfrak{C}$-zone: the preferably rotation of the SC implements about the transversal axes *Ox*, but the angle of intrinsic rotation fulfills the periodical oscillations around the value $\varphi^*=3\pi/2$ (i.e. the SC main body is turned by the other side in the comparison with the $\mathfrak{C}$-zone). The type of motion in the $\mathfrak{D}$-zone, like the previous $\mathfrak{C}$-zone motion, is the undesirable regime for the spin-stabilized SC.

The $\mathfrak{H}$-zone appears in the phase portrait only at the action of the perturbations and covers itself the parts of areas of all main zones ($\mathfrak{A}-\mathfrak{D}$). The $\mathfrak{H}$-zone is filled by split heteroclinic trajectories, generating the heteroclinic net and chaotic layer. All incoming into this zone phase trajectories fulfill complicated motion passing through covered parts of the main zones. Therefore, the corresponding dynamics of the SC in the $\mathfrak{H}$-zone alternates in the time the properties of all main zones ($\mathfrak{A}-\mathfrak{D}$).

As we already indicated, the most important and applicable for the gyrostat-satellite zone is the $\mathfrak{A}$-zone where the longitudinal axes of the SC is oriented and spin-stabilized in the direction of the angular momentum vector **K**.

The satellite can take at the launching (at the separating from the upper stage) the arbitrary spatial orientation and can proceed to the attitude motion in any phase zone ($\mathfrak{A}-\mathfrak{D}$). Therefore, it is very important to change the initial phase zone of the SC motion, and to move the dynamics into the necessary phase zone (and mainly into the $\mathfrak{A}$-zone). The change of the SC dynamics, certainly, can be realized by many ways and with the help of different actuators. In this research, this task is solved by the way of the creation of the heteroclinic chaos with the entering phase trajectories into the $\mathfrak{H}$-zone and exiting from it in the target-area. Then from the main scheme of the chaos-hub method (fig.1) the following detailed algorithm can be constructed:

1. The SC realizes the initial regime of the free angular motion.
2. The control system begins to create the constant spin-up/spin-down torque by the internal rotor-engine, that increase/decrease angular velocity of the rotor and of the main body until the heteroclinic regime will be achieved (it can be defined by a specific criterion).
3. The control system switches to the creation of the small harmonic perturbations (by the internal rotor-engine and/or by the magnetic actuator) to generate and to support the heteroclinic chaos. The SC realizes the chaotic motion with monitoring the current dynamical parameters waiting for the arrival of the phase trajectory into the target-zone of the phase space through the chaotic layer (it can be defined by specific criteria).
4. After the arrival of the phase trajectory into the target zone, the control system immediately stops the perturbations, then the heteroclinic chaos vanishes, and the SC dynamics proceeds to the new regular regime in the target-zone of the phase space.
5. (This step can be realized optionally) If it is needed to move up/down the new regular phase trajectory relatively the phase portrait, we can fulfill the step #2 in its back direction.

Now we should give some explanations to the implementation of the algorithm steps.

The *step #1* corresponds to the natural initial regular motion of the SC, and there is not additional aspects to underline.

In the framework of the *step #2*, the internal constant torque is initiated in the unperturbed system to change the current regime on the heteroclinic one. This piecewise constant torque is applied to the rotor-

body with the aim of spin-up/spin-down its angular velocity, and to move the separatrixes area up/down on the phase portrait:

$$\dot{\Delta} = M_{spin} \cdot \left(H\left(t - t_{ini}\right) - H\left(t - t_{hetero}\right) \right) \tag{4.1}$$

where M_{spin} – is the constant, $H(t)$ – the Heaviside function, t_{ini} is the time-point of the start of maneuver realization, t_{hetero} – the time-point of the heteroclinic regime achievement. It is clear, that on the time-interval [t_{ini}, t_{hetero}] the angular momentum of the rotor-body varies linearly $\left(\Delta(t) = \Delta_{ini} + M_{spin} \cdot t\right)$, which simultaneously changes the phase portrait [18]. If we consider the series of small separated steps with the graceful changing the Δ-value, then we see, that during the Δ-value increasing/decreasing the separatrix-region will gradually moving up/down at the phase portrait (e.g., it is presented at fragments (fig.5-a, -c, -e) as the rising heteroclinic zone at the Δ-value increasing). Moreover, at the "critical" increasing the Δ-value [18] the heteroclinic region is raised up to the border level (L/I_2=1) of the phase portrait (fig.5-e); and analogously, at the "critical" decreasing the Δ-value [18] the heteroclinic region is mowed down on the border level (L/I_2= -1) of the phase portrait (fig.5-g). Therefore, the heteroclinic zone ($\mathfrak{H}$-zone) can be moved to the appropriate level corresponding to the initial regime (L_0/I_2) by the simple way, i.e. by the spin-up/spin-down of the rotor with the help of the action of pricewise constant torque. In other words, by this way we can create the heteroclinic region in any necessary phase space area. So, it is possible to implement changing any initial regime to the heteroclinic one, and fully realize the step #2 of the algorithm.

Here it is important to indicate, that the time-point t_{hetero} is not the predefined value – it must be identified by the control system during the rotor spin-up/spin-down process. This identification is based on the condition fulfilling, when the values of the angular velocity components satisfy to heteroclinic phase trajectories; and, as it follows from the analytical solutions [17], this time-point will be defined by the criterion:

$$if \left\{ \left\| r(t) - \frac{\Delta(t)}{B - C_b} \right| - \left| p(t) \cdot \sqrt{\frac{A(A-B)}{C_b(B-C_b)}} \right\| \le \xi \right\} \ then \ t \to t_{hetero} \tag{4.2}$$

where ξ is an acceptable small "proximity" $\left(0 < \xi << 1\right)$ of the current phase trajectory to the unperturbed separatrix, which can be selected as the precision parameter at the control system development.

The *step #3* is fulfilled after initiation of the SC motion close (with the small proximity ξ) to the unperturbed heteroclinic dynamics. This step represents the perturbed motion at the action of the internal and/or external (magnetic) perturbations – this perturbed dynamics already was described mathematically in the section 2 and considered numerically in the section 3. As it is formulated above (1.8), the perturbations start their own action at the t_{start} time-point ($t_{start} > t_{hetero}$) and operate until the time-point t_{finish}. In this time-interval [t_{start}, t_{finish}] the SC implements the chaotic motion in the $\mathfrak{H}$-zone and the control system monitors the current dynamical parameters in each time-point with checking the entry criteria for the target-zone. The entry conditions can be obtained from the analytical consideration of the heteroclinic trajectories [17] with the analysis of the geometry of the polhodes location (fig.7-b).

For the $\mathfrak{A}$-zone the entry criteria are:

$$\begin{cases} \left| r(t) - \dfrac{\Delta(t)}{B - C_b} \right| > \left| p(t) \cdot \sqrt{\dfrac{A(A-B)}{C_b(B-C_b)}} \right|; \\ r(t) - \dfrac{\Delta(t)}{B - C_b} > 0 \end{cases} \tag{4.3}$$

For the $\mathfrak{B}$-zone the entry criteria are:

$$\begin{cases} \left| r(t) - \dfrac{\Delta(t)}{B - C_b} \right| > \left| p(t) \cdot \sqrt{\dfrac{A(A-B)}{C_b(B-C_b)}} \right|; \\ r(t) - \dfrac{\Delta(t)}{B - C_b} < 0 \end{cases} \tag{4.4}$$

For the $\mathfrak{C}$-zone the entry criteria are:

$$\begin{cases} \left| r(t) - \dfrac{\Delta(t)}{B - C_b} \right| < \left| p(t) \cdot \sqrt{\dfrac{A(A-B)}{C_b(B-C_b)}} \right|; \\ p(t) > 0 \end{cases} \tag{4.5}$$

For the $\mathfrak{D}$-zone the entry criteria are:

$$\begin{cases} \left| r(t) - \dfrac{\Delta(t)}{B - C_b} \right| < \left| p(t) \cdot \sqrt{\dfrac{A(A-B)}{C_b(B-C_b)}} \right|; \\ p(t) < 0 \end{cases} \tag{4.6}$$

The fulfillment of the entry criteria for the necessary target-zone defines the time-point t_{finish} when the heteroclinic chaos should be immediately stopped.

The *step #4* corresponds to immediately disabling the perturbations at the defined time-point t_{finish}. After that, the SC will implement the final regular regime in the target-zone of the phase space.

6. The numerical modelling of the chaos-hub method implementation

In this section, we present the numerical modelling of the chaos-hub method, which used the algorithm described in the section 5 in all details. In this section three cases of the reorientation are demonstrated: the case "$\mathfrak{CHA}$" of the passage to the final main $\mathfrak{A}-$zone through the chaos-hub (the $\mathfrak{H}-$zone) starting from the initial main $\mathfrak{C}-$zone (fig.8); the case "$\mathfrak{BHA}$" of the passage to the final main $\mathfrak{A}-$zone through the chaos-hub starting from the initial main $\mathfrak{B}-$zone (fig.9); the case "$\mathfrak{AHC}$" of the passage to the final main $\mathfrak{C}-$zone through the chaos-hub starting from the initial main $\mathfrak{A}-$zone (fig.10). The corresponding values of the parameters are indicated in the table (tabl.2). All cases use the external magnetic perturbations to the chaos-hub creation, that, certainly, could also be easy fulfilled with help of the internal perturbation in the rotor-body spin-up-engine. For all calculations the common parameters

are selected: b_x=b_y=0; μ_Δ,=0 [N*m]; A=20, B=15, C_b, =6 [kg*m^2]. For the considerations convenience the step of the chaos-hub initiating in all calculations begins at the t_{start}=0 for all cases.

Let us firstly to show the numerical time-dependencies for the angular motion parameters at the passage "ℭℌ𝔄" (Fig.8). At the fragment (fig.8-a) is depicted the time-history of the nutation angle, where color areas indicate the main stages of the algorithm implementation:

1. The gray area corresponds to the initial regular regime (in the ℭ-zone), started its own realization at the time t_0.

2. The blue area coincides with the time-interval [t_{ini}, t_{hetero}] of the action of the spin-down torque (the value M_{spin} is negative) to arrive into the heteroclinic region.

3. The pink area represents the motion in the unperturbed heterolinic regime during the time-interval [t_{hetero}, t_{start}].

4. At the time-point t_{start} the activation of the perturbation is executed, and then the chaotic dynamics of the SC realizes in the created ℌ-zone until the control system generates the command to exit from the heteroclinic chaos at the time-point t_{finish} when the criterion (4.3) is fulfilled – this wandering in the chaos is corresponded to the yellow area (also this chaotic phase trajectory is separately plotted at the fragment fig.8-e).

5. Immediately after the time-point t_{finish} the SC will realize the new regular regime in the 𝔄-zone, that is depicted as the green area.

In the fragment (fig.8-f) the control chart for selecting the t_{finish} time-point is shown, where light-green rectangular pulses correspond to the time-intervals of the fulfillment of the criterion (4.3) during the implementation of the chaotic wandering in the ℌ-zone. Inside such time-intervals the control system can select any time-point to jump from the heteroclinic chaos into new regular regimes in the 𝔄-zone; after this jump the dynamics always realizes in the target-zone.

Fragments (fig.8-b, -c, -d) contain the time-histories for the angular velocity components.

The analogous parameters time-histories for the passages "𝔅ℌ𝔄" and "𝔄ℌℭ" are presented at the figures fig.9 and fig.10, where also the time-dependencies $\varphi(t)$ and $\psi(t)$ are shown (fragments "e").

Table 2. *Parameters of the chaos-hub method implementation*

Case	θ_0, rad	φ_0, rad	ψ_0, rad	p_0, 1/s	q_0, 1/s	r_0, 1/s	Δ_{ini}, kg*m^2/s	M_{spin}, N*m	t_0, s	t_{ini}, s	t_{hetero}, s	t_{start}, s	t_{finish}, s	$\mu_z Bz$, N*m	Ω_z, 1/s
ℭℌ𝔄	1.59	-0.98	-0.64	0.48	5.01	-0.46	1	-0.15	-50	-30	-25	0	66	2	3
𝔅ℌ𝔄	1.86	0.18	-0.07	3.33	1.93	-5.72	12.75	-0.5	-70	-50	-25	0	60	1	0.75
𝔄ℌℭ	1.33	-0.12	-0.80	-2.52	3.58	7.12	-24.75	1	-70	-50	-25	0	40	1	0.75

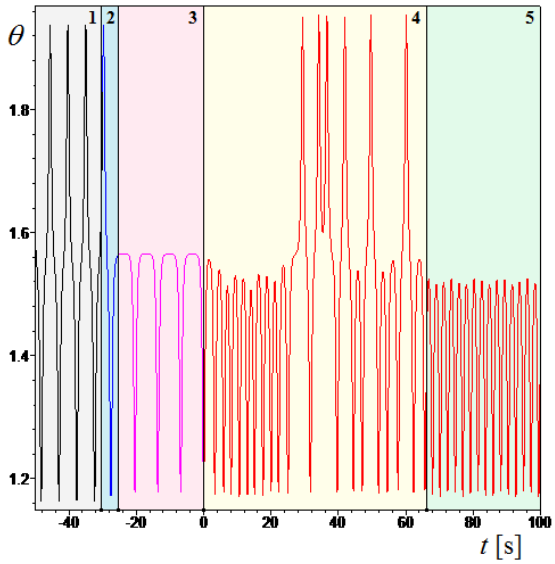

(a)

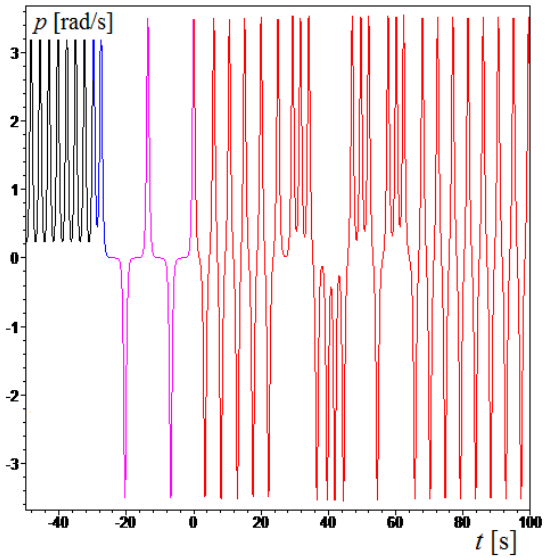

(b)

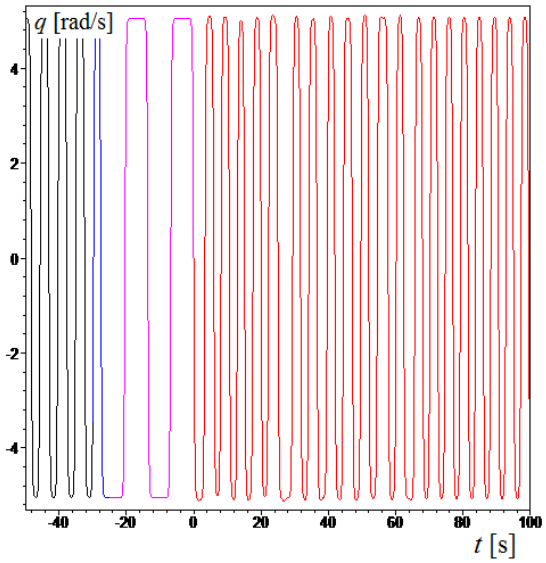

(c)

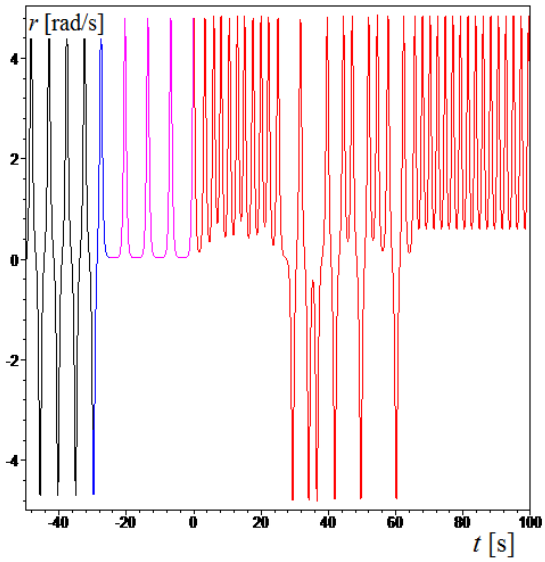

(d)

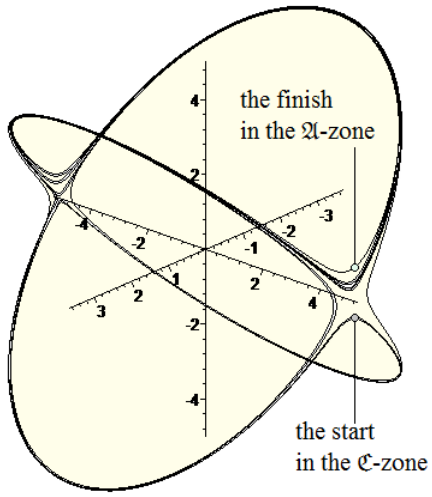

(e)

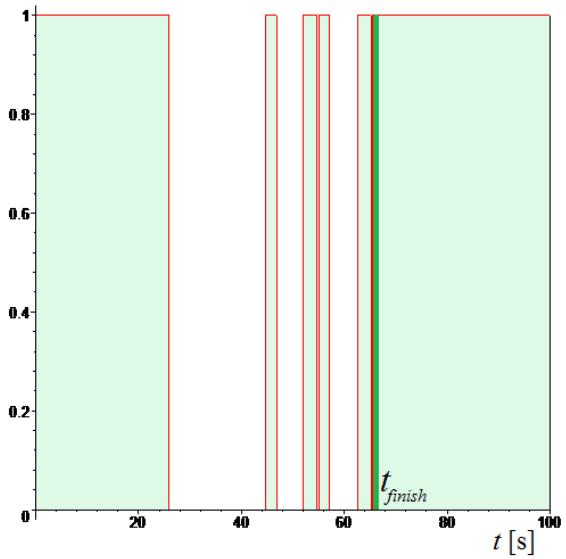

(f)

Fig.8 – *The case ЄЋЯ of the SC attitude reorientation modeling*

PREPRINT 10.1016/j.cnsns.2017.11.008

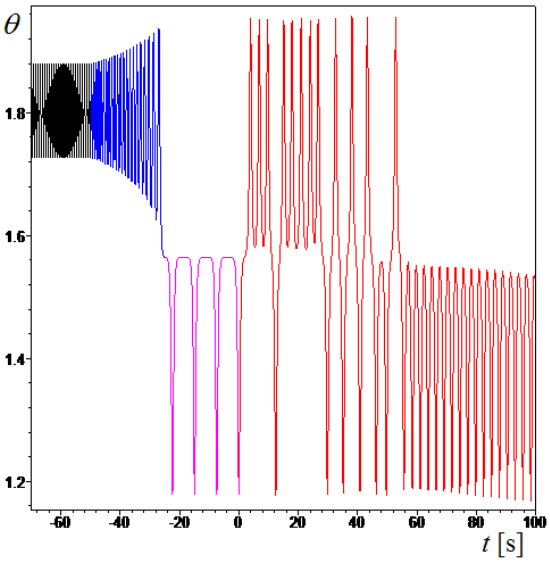

(a)

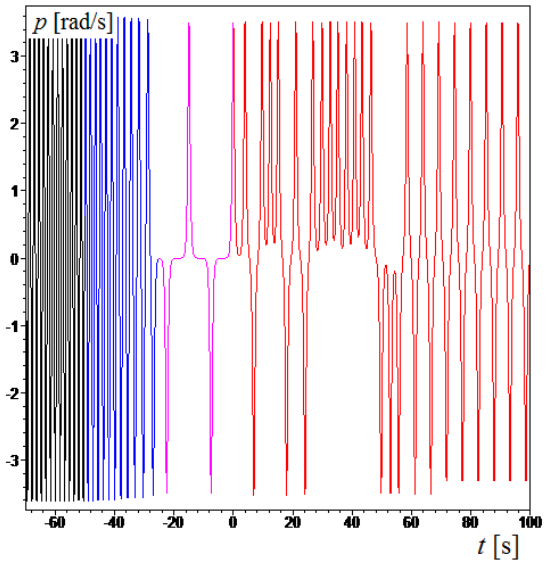

(b)

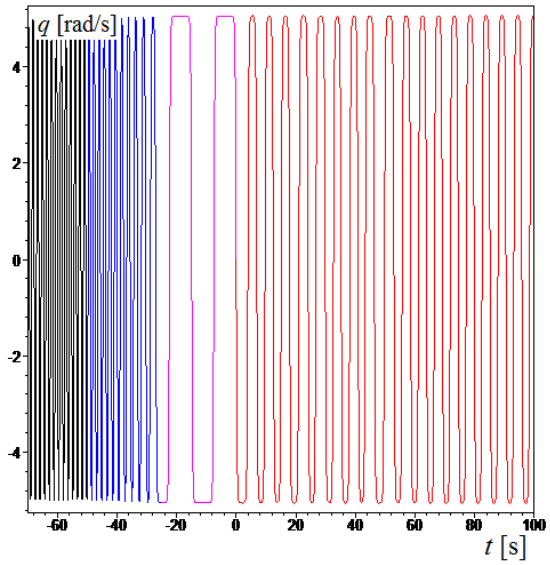

(c)

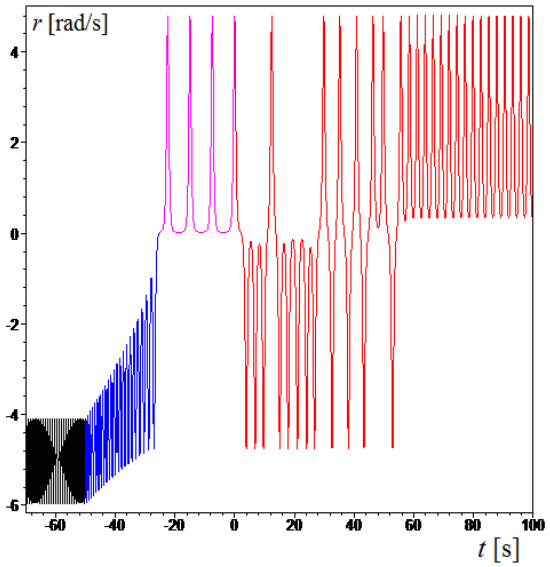

(d)

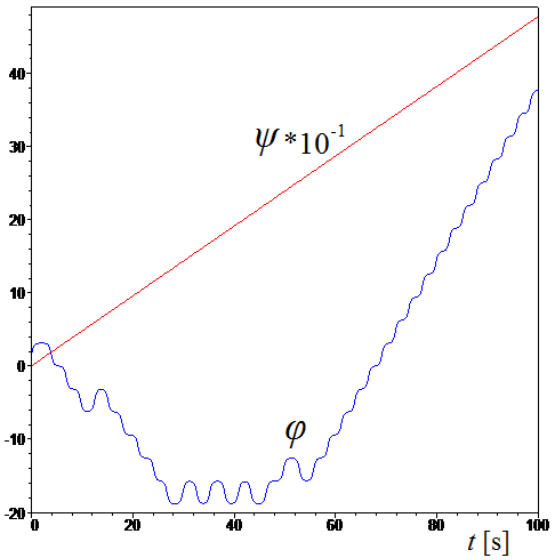

(e)

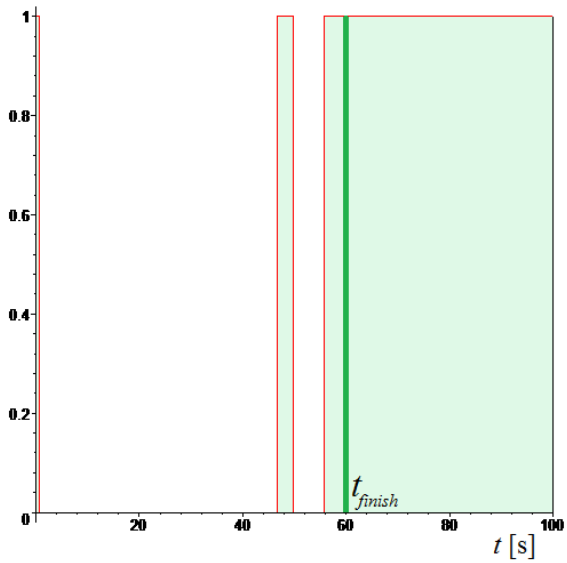

(f)

Fig.9 – *The case ЭНА of the SC attitude reorientation modeling*

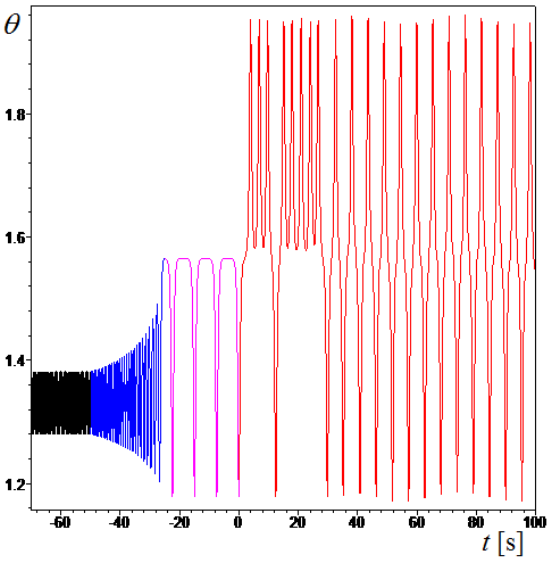

(a)

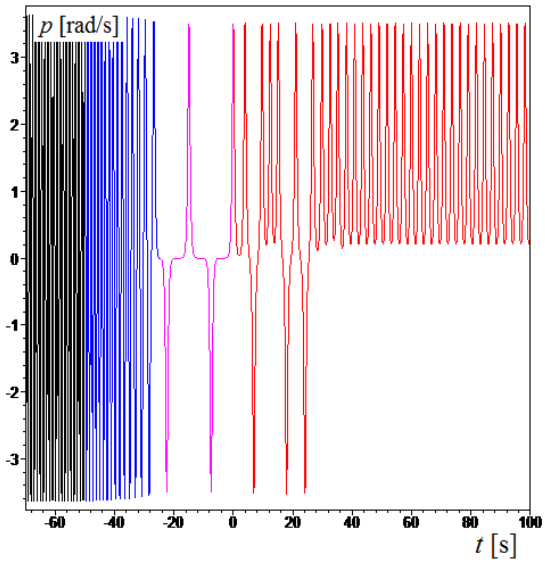

(b)

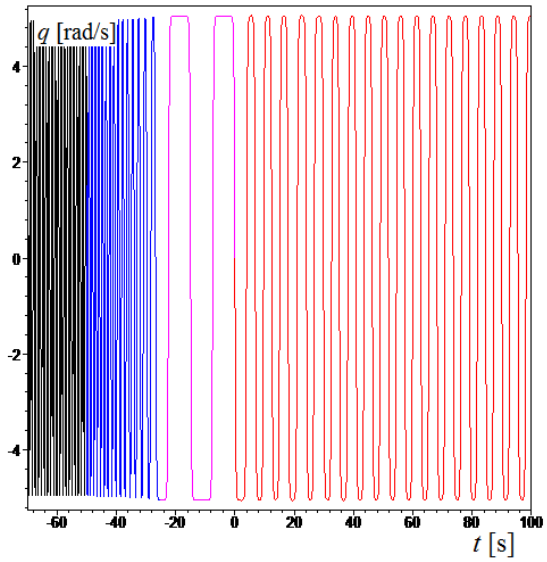

(c)

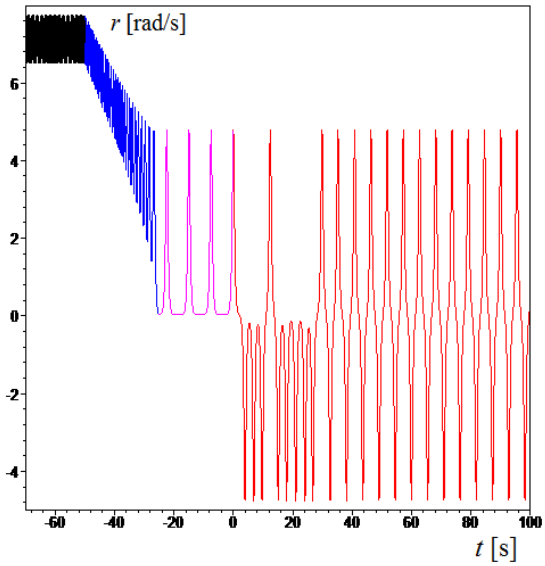

(d)

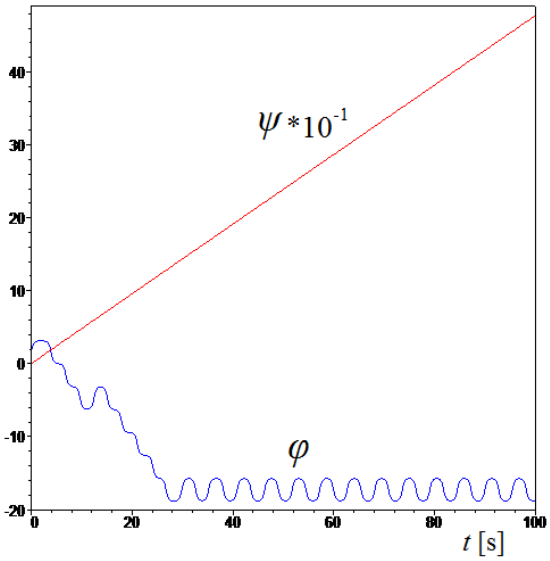

(e)

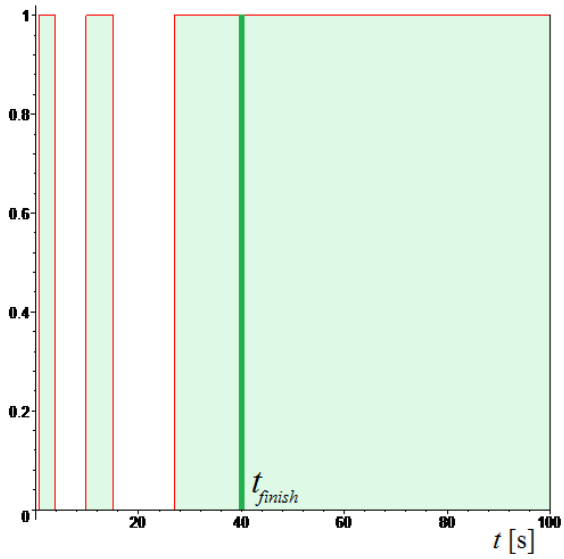

(f)

Fig.10 – *The case* $\mathfrak{AHC}$ *of the SC attitude reorientation modeling*

Conclusion

In this work, the chaos was explored as the positive phenomenon, which allows to change systems dynamics using the ability of the chaos to fill the available areas of systems phase space, and to interconnect the dynamical zones with the different behavior. These dynamical opportunities of the chaos arise due to phase trajectories mixing and infinite increasing distances between them. Such properties allow to consider the chaos as the hub of systems dynamics, linking the different areas of the phase space.

In particular, the heteroclinic chaos was investigated in this paper as the instrument of the spacecraft attitude dynamics changing. The developed method of the spacecraft attitude control is based on the transfer of the dynamical regime close to the heteroclinic phase orbit (separatrix) with the subsequent intentional creation of the perturbations. These perturbations split the heteroclinic trajectories and generate the heteroclinic chaos. The perturbations are created by the control system with help of available actuators. At the fulfillment of necessary criteria, the control systems terminates the intentional perturbations and eliminates the chaos, and the spacecraft jumps from the chaos into new phase target-regime.

As the actuators in this research the internal rotor with the electromotor and the magnetic torquer were considered. The simplicity of these types of actuators defines the possibility of real applications of the chaotic control scheme as attitude control systems even for simplest and smallest types of spacecraft, including nanosatellites. Moreover, this simple “chaotic” control can be used as the reserve scheme for parrying irregular motion modes and accidents. In any case, the described positive technical application of the chaos to the problem of the space flight has all the rights to its existence and to its further development.

Summarizing all of the above, we can conclude, that different aspects of the chaos are very important not only for the fundamental (philosophical, physical and mathematical) point of view, but also are significant for the technical applications, including the problem of the spacecraft attitude dynamics and control.

Acknowledgments

This work is partially supported by the Russian Foundation for Basic Research (RFBR#15-08-05934-A), and by the Ministry education and science of the Russian Federation in the framework of the State Assignments to higher education institutions and research organizations in the field of scientific activity - the project # 9.1616.2017/ПЧ (9.1616.2017/4.6).

References

[1] Andronov, A.A., Vitt, E.A. and Khaiken, S.E. (1966). Theory of Oscillators (Pergamon, New York).

[2] Anishchenko, V.S., Astakhov, V., Neiman, A., Vadivasova, T., & Schimansky-Geier, L. (2007). Nonlinear dynamics of chaotic and stochastic systems: tutorial and modern developments. Springer Science & Business Media.

[3] Arnold V.I. (1964). Instability of dynamical systems with several degrees of freedom, Doklady Akademii Nauk SSSR, 156 (1), pp. 9-12.

[4] Arnold, V.I. (1963). Proof of AN Kolmogorov's theorem on the conservation of conditionally periodic motions with a small variation in the Hamiltonian. Russian Math. Surv, 18(9).

[5] Arnold, V.I. (1968). The stability problem and ergodic properties for classical dynamical systems. In Vladimir I. Arnold-Collected Works. Springer Berlin Heidelberg, pp. 107-113.

[6] Arnold, V.I., Kozlov, V.V. and Neishtadt A.I. (1988). Mathematical Aspects of Classical and Celestial Mechanics (Springer, New York).

[7] Aslanov, V. S. (2015). Chaotic behavior of a body in a resistant medium. International Journal of Non-Linear Mechanics, 73, 85-93.

[8] Aslanov, V.S. (2015). Chaos Behavior of Space Debris During Tethered Tow. Journal of Guidance, Control, and Dynamics, 2399-2405.

[9] Aslanov, V.S., & Doroshin, A.V. (2010). Chaotic dynamics of an unbalanced gyrostat. Journal of Applied Mathematics and Mechanics, Volume 74, Issue 5, pp.525-535.

[10] Bao-Zeng, Y. (2011). Study on the Chaotic Dynamics in Attitude Maneuver of Liquid-Filled Flexible Spacecraft, AIAA Journal, Vol. 49, No. 10, pp. 2090-2099.

[11] Bao-Zeng, Y., Jiafang X. (2007). Chaotic attitude maneuvers in spacecraft with a completely liquid-filled cavity, Journal of Sound and Vibration 302, pp. 643–656.

[12] Beletskiĭ, V.V., Pivovarov, M.L., & Starostin, E.L. (1996). Regular and chaotic motions in applied dynamics of a rigid body. Chaos: An Interdisciplinary Journal of Nonlinear Science, 6(2), 155-166.

[13] Boccaletti, S., Grebogi, C., Lai, Y. C., Mancini, H., & Maza, D. (2000). The control of chaos: theory and applications. Physics reports, 329(3), pp. 103-197.

[14] Boccaletti, S., Kurths, J., Osipov, G., Valladares, D.L., Zhou, C.S. (2002). The synchronization of chaotic systems. Physics Reports 366, pp. 1–101.

[15] Chen Li-Qun, Liu Yan-Zhu (2002). Chaotic attitude motion of a magnetic rigid spacecraft and its control, International Journal of Non-Linear Mechanics 37, pp. 493–504.

[16] Chen, H.K., & Lee, C.I. (2004). Anti-control of chaos in rigid body motion. Chaos, Solitons & Fractals, 21(4), pp. 957-965.

[17] Doroshin, A.V. (2012). Heteroclinic dynamics and attitude motion chaotization of coaxial bodies and dual-spin spacecraft. Communications in Nonlinear Science and Numerical Simulation, 17 (3), pp. 1460-1474.

[18] Doroshin, A.V. (2014). Chaos and its avoidance in spinup dynamics of an axial dual-spin spacecraft. Acta Astronautica, 94 (2), pp. 563-576.

[19] Doroshin, A.V. (2015). Attitude Control and Angular Reorientations of Dual-Spin Spacecraft and Gyrostat-Satellites Using Chaotic Regimes Initiations, Lecture Notes in Engineering and Computer Science: Proceedings of The World Congress on Engineering 2015, 1-3 July, 2015, London, U.K., pp100-104.

[20] Doroshin, A.V. (2016). Initiations of chaotic motions as a method of spacecraft attitude control and reorientations. IAENG Transactions on Engineering Sciences: pp. 15-28.

[21] Doroshin, A.V. (2017). Attitude dynamics of gyrostat-satellites under control by magnetic actuators at small perturbations, Communications in Nonlinear Science and Numerical Simulation 49, pp.159–175.

[22] El-Gohary Awad (2005). Optimal control of damping rotation of a rigid body using fly wheels with friction, Chaos, Solitons and Fractals 24, pp. 207–221.

[23] El-Gohary Awad (2009). Chaos and optimal control of steady-state rotation of a satellite-gyrostat on a circular orbit, Chaos, Solitons & Fractals, Volume 42, pp. 2842-2851.

[24] Guckenheimer, J., & Holmes, P.J. (1983). Nonlinear oscillations, dynamical systems, and bifurcations of vector fields. Vol. 42. Springer Science & Business Media.

[25] Holmes, P.J. (1990). Poincaré, celestial mechanics, dynamical-systems theory and chaos – Physics Reports (Review Section of Physics Letters) 193, No. 3, pp. 137—163 (North-Holland).
[26] Holmes, P.J., & Marsden, J.E. (1983), Horseshoes and Arnold diffusion for Hamiltonian systems on Lie groups, Indiana Univ. Math. J. 32, pp. 273-309.
[27] Iñarrea, M. (2009). Chaos and its control in the pitch motion of an asymmetric magnetic spacecraft in polar elliptic orbit, Chaos, Solitons & Fractals,Volume 40, Issue 4, pp.1637-1652.
[28] Iñarrea, M., and Lanchares, V. (2000). Chaos in the reorientation process of a dual-spin spacecraft with time-dependent moments of inertia, Int. J. Bifurcation and Chaos. 10, pp. 997-1018.
[29] Iñarrea, M., Lanchares, V., Rothos, V. M., Salas, J. P. (2003). Chaotic rotations of an asymmetric body with timedependent moment of inertia and viscous drag, International Journal of Bifurcation and Chaos, Vol. 13, No. 2, pp. 393-409.
[30] Ivanov, D.S., Ovchinnikov, M.Y., Penkov, V.I., Roldugin, D.S., Doronin, D.M., & Ovchinnikov, A.V. (2017). Advanced numerical study of the three-axis magnetic attitude control and determination with uncertainties. Acta Astronautica, 132, 103-110.
[31] Kolmogorov, A.N. (1954) On conservation of conditionally periodic motions for a small change in Hamilton's function. Dokl. Akad. Nauk SSSR, 98, 527-530.
[32] Kozlov, V.V. (1980). Methods of Qualitative Analysis in the Dynamics of a Rigid Body, Gos. Univ., Moscow.
[33] Kozlov, V.V. (1983). Integrability and non-integrability in Hamiltonian mechanics. Russian Mathematical Surveys, 38(1).
[34] Kuang Jinlu, Tan Soonhie, Arichandran Kandiah, Leung A.Y.T. (2001), Chaotic dynamics of an asymmetrical gyrostat, International Journal of Non-Linear Mechanics 36, pp. 1213-1233.
[35] Kuang, J.L., Meehan, P.A., Leung, A.Y.T. (2006), On the chaotic rotation of a liquid-filled gyrostat via the Melnikov–Holmes–Marsden integral, International Journal of Non-Linear Mechanics 41, pp. 475 – 490.
[36] Kuang, J.L., Meehan, P.A., Leung, A.Y.T. (2006), Suppressing chaos via Lyapunov–Krasovskii's method, Chaos, Solitons and Fractals 27, pp. 1408–1414.
[37] Kuznetsov, N.V., & Leonov, G.A. (2016). Strange Attractors and Classical Stability Theory: Stability, Instability, Lyapunov Exponents and Chaos. Handbook of Applications of Chaos Theory. Chapman and Hall/CRC, pp. 105-134.
[38] Kuznetsov, S.P. (2012). Hyperbolic Chaos: A Physicist's View. Higher Education Press, Beijing and Springer-Verlag GmbH Berlin Heidelberg.
[39] Leonov, G.A., & Kuznetsov, N.V. (2013). Hidden attractors in dynamical systems. From hidden oscillations in Hilbert–Kolmogorov, Aizerman, and Kalman problems to hidden chaotic attractor in Chua circuits. International Journal of Bifurcation and Chaos, 23(01), 1330002.
[40] Leung, A. Y. T., Kuang, J. L. (2004), Spatial chaos of 3-D elastica with the Kirchhoff gyrostat analogy using Melnikov integrals, Int. J. Numer. Meth. Eng. 61, pp.1674–1709.
[41] Leung, A.Y.T., Kuang, J.L. (2007), Chaotic rotations of a liquid-filled solid, Journal of Sound and Vibration 302, pp. 540–563
[42] Lichtenberg, A.J., and Lieberman, M.A. (1983). Regular and stochastic motion. Vol. 38. Springer Science & Business Media.
[43] Lorenz, E.N. (1963). Deterministic nonperiodic flow, J. Atmos. Sci. 20, pp.130–141.
[44] Lovera, M., Astolfi, A. (2004). Spacecraft attitude control using magnetic actuators, Automatica 40, pp.1405 – 1414.

[45] Melnikov, V.K. (1963), On the stability of the centre for time-periodic perturbations, Trans. Moscow Math. Soc. No.12, pp. 1-57.
[46] Moser, J. (1962). On invariant curves of area-preserving mappings of an annulus. Nachr. Akad. Wiss. Göttingen Math.-Phys. Kl. II, 1-20.
[47] Moser, J. (1973). Stable and Random Motions in Dynamical Systems, Princeton Univ. Press, Princeton.
[48] Or, A.C. (1998). Chaotic Motions of a Dual-Spin Body, Transactions of the ASME, Vol.65, pp. 150-156.
[49] Pecora, L.M., Carroll, T.L., Johnson, G.A., Mar, D.J. (1997), Fundamentals of synchronization in chaotic systems, concepts, and applications. Chaos 7 (4), pp. 520-543.
[50] Peng, J., & Liu, Y. (2000), Chaotic motion of a gyrostat with asymmetric rotor, International Journal of Non-Linear Mechanics, Volume 35, Issue 3, pp. 431-437.
[51] Poincaré, H. (1899), Les Methodes Nouvelles de La Mécanique Celeste, Vols. 1-3 (Gauthier Villars, Paris).
[52] Silani, E., & Lovera, M. (2005). Magnetic spacecraft attitude control: a survey and some new results, Control Engineering Practice 13, pp. 357–371.
[53] Sprott, J.C. (2003). Chaos and time-series analysis. Vol. 69. Oxford: Oxford University Press.
[54] Strogatz, S. H. (2014). Nonlinear dynamics and chaos: with applications to physics, biology, chemistry, and engineering. Westview press.
[55] Tabor, M. (1989). Chaos and integrability in nonlinear dynamics. Wiley.
[56] Thompson, J. M. T., & Stewart, H. B. (2002). Nonlinear dynamics and chaos. John Wiley & Sons;
[57] Wiggins, S. (1988), Global Bifurcations and Chaos: Analytical Methods (Applied mathematical sciences: vol. 73). Springer-Verlag.
[58] Wiggins, S. (1990), Introduction to applied nonlinear dynamical systems and chaos. Springer-Verlag.
[59] Wiggins, S. (1992), Chaotic Transport in Dynamical Systems. Springer-Verlag.
[60] Wiggins, S. (2003). Introduction to applied nonlinear dynamical systems and chaos. Vol. 2. Springer Science & Business Media.